Optical Lock-in Spectrometry Reveals Useful Spectral Features of Temporal Light Modulation in Several Light Source Technologies

Christophe Martinsons, Nicolas Picard, Samuel Carré

Author's version of the following published article:
Martinsons C, Picard N, and Carré S. "Optical Lock-in Spectrometry Reveals Useful Spectral Features of Temporal Light Modulation in Several Light Source Technologies." *LEUKOS*, June 22, 2022, 1–19. https://doi.org/10.1080/15502724.2022.2077754.

Optical lock-in spectrometry reveals the spectral features of temporal light modulation in several light source technologies

Christophe Martinsons *, Nicolas Picard and Samuel Carré

Division of Acoustics, Vibrations, Lighting and Electromagnetic Fields
Centre Scientifique et Technique du Bâtiment, Saint Martin d'Hères and Nantes, France

***Corresponding author**

christophe.martinsons@cstb.fr

ORCID

S. Carré: http://orcid.org/0000-0002-0484-2331
C. Martinsons: http://orcid.org/0000-0002-2286-5991

Abstract

This paper presents a study of the spectral characteristics of temporal light modulation of several technologies of lighting products. An optical lock-in spectrometer was designed for this purpose and integrated in a spectral radiant flux measurement facility. It was applied to incandescent and fluorescent lamps, as well as lamps based on white phosphor-converted LEDs and tunable RGB LEDs.

The results are well correlated with the light emission processes of each technology. For incandescent lamps, the spectral modulation follows a $1/\lambda$ relationship in agreement with the blackbody radiation laws. Measurements performed on halophosphate and tri-phosphor tubes agree well with published data. The modulation and phase spectra of fluorescent lamps reveal a variable modulation rate across the visible range, directly related to the fluorescence lifetimes of the different luminophores, which were estimated from our data using a model of single exponential decay.

The spectral modulation of white phosphor-converted LED lamps is nearly constant across the visible spectrum, demonstrating that their color parameters can be assessed from the lock-in modulation amplitude spectrum. In the case of tunable RGB LED lamps using PWM, the spectral modulation widely differs from the steady-state spectral distribution and changes with the user settings, confirming the possible occurrence of temporal color artifacts.

Optical lock-in spectrometry instruments can be used to improve spectral and color measurements of solid-state lighting, opening new opportunities for laboratory and remote sensing applications. Other foreseeable applications of optical lock-in spectrometry are also presented.

Keywords

Lighting, optical lock-in detection, temporal light modulation, spectral modulation, photometry, spectroradiometry, temporal color modulation, color flicker

Author's version of the following published article:
Martinsons C, Picard N, and Carré S. "Optical Lock-in Spectrometry Reveals Useful Spectral Features of Temporal Light Modulation in Several Light Source Technologies." *LEUKOS*, June 22, 2022, 1–19. https://doi.org/10.1080/15502724.2022.2077754.

1. Introduction

Temporal light modulation (TLM) is a change in the luminous quantity or spectral distribution of light with respect to time of a light source or a lighting system. These changes arise because of the electrical design of the light source power supply or in the presence of fluctuations in the electrical distribution network (CIE 2016). The exposure to temporal light modulation may cause undesired effects on visual performance and health (Veitch et al. 2021) (Sekulovski et al. 2019). The term "temporal light artefacts" (TLA) is related to the effects that TLM induce on human vision (CIE 2016) (CIE 2022).

Three types of TLAs are commonly reported in general lighting applications: flicker, the stroboscopic effect and the phantom array (CIE 2022). When the spectral power distribution of the light changes with time, color temporal artefacts may occur. Chromatic flicker (Van der Horst 1969) is an example of color temporal artifact defined by the perception of the changing color of a light source in static conditions. In non-static conditions, different instances of color artefacts may occur, generally known as color breakup. Color breakup is frequently seen in displays presenting colors sequentially (Johnson, Kim, and Banks 2014). It can be associated with the stroboscopic effect in the case of viewing a moving object under spectrally modulated light (Bullough and Skinner 2019). In the case of an observer viewing a spectrally modulated light source while doing eye saccades, color breakup can be seen in association with the phantom array effect (Johnson, Kim, and Banks 2014).

Very little spectral modulation data have been published in the field of lighting. In 1990, Wilkins and Clark published this type of data for fluorescent tubes that are now obsolete (Wilkins and Clark 1990). To the best of our knowledge, their work has never been replicated nor extended to modern fluorescent lamps and LEDs. A new spectrometry technique was designed for this purpose and is described for the first time in this paper. The technique is based on an optical implementation of lock-in detection. The new instrument was applied to common types of indoor light sources, including "legacy" lighting technologies to provide a validation of the experimental results.

2. Principle of operation

Lock-in detection is a well-established technique to measure the amplitude and phase of a modulated electrical signal in the presence of multiple frequency components, a non-stationary background and other forms of noise (Zurich Instrument 2016). It uses a sine wave reference

Author's version of the following published article:
Martinsons C, Picard N, and Carré S. "Optical Lock-in Spectrometry Reveals Useful Spectral Features of Temporal Light Modulation in Several Light Source Technologies." *LEUKOS*, June 22, 2022, 1–19. https://doi.org/10.1080/15502724.2022.2077754.

waveform whose frequency and phase must be locked to the modulated component of the signal to measure.

Lock-in detection first proceeds by routing the signal to two channels working in parallel. In the first channel, the in-phase channel, the signal is multiplied by the reference waveform. In the second channel, the quadrature channel, the signal is multiplied by the same reference waveform but phase-shifted by 90°. After the multiplier stages, both signals are sent to identical low pass filters. Following the low pass filtering stage, the output of both channels are respectively the real and imaginary parts of the Fourier component of the signal at the exact reference frequency. The outputs of the in-phase channel and the quadrature channel can be combined to give the amplitude and phase of the signal at the reference frequency. Lock-in detection can be seen as a very narrow phase-sensitive bandpass filter centered on the reference frequency, rejecting the dc component and components modulated at other frequencies (Zurich Instrument 2016).

In the field of spectrometry, commercially available lock-in amplifiers are used to improve the signal to noise ratio of spectra obtained with single photodetectors and modulated light sources. This is the case of analytical spectrometry based on scanning grating spectrometers (Wang et al. 2017) and Raman spectrometry using modulated pump laser beams (Ragni et al. 2018). When using array spectrometers, the use of lock-in detection is complicated because the electrical signals given by the pixels of the detector array should be processed independently and simultaneously. Commercial lock-in amplifiers may have up to a few tens of measurement channels, but this number falls short of the typical number of spectral points given by array spectrometer. The smallest number of spectral data used in spectrophotometry is about 400 (380 nm to 780 nm by step of 1 nm) but may increase to 4000 when a spectral resolution of 0.1 nm is used, as it is the case when measuring the lines of discharge lamps.

To make lock-in detection possible with detector arrays having many pixels, the same principles can be applied to the optical signal itself. This can be achieved by replacing the multiplier stage by an optical modulator. This approach enables the parallel and synchronous processing of all the pixels simultaneously. An optical lock-in spectrometer equipped with a 2D focal plane array and an acousto-optic deflector was described in (Fodor, Rothenberger, and Jevy 2005). It was designed to perform time-resolved absorption measurements of quantum dots and nanocrystals excited by a modulated near-infrared diode laser. However, this technique required to run a computer-intensive digital image processing algorithm in real-time to extract the amplitude and phase absorption

Author's version of the following published article:
Martinsons C, Picard N, and Carré S. "Optical Lock-in Spectrometry Reveals Useful Spectral Features of Temporal Light Modulation in Several Light Source Technologies." *LEUKOS*, June 22, 2022, 1–19. https://doi.org/10.1080/15502724.2022.2077754.

spectra. Optical lock-in detection has been recently applied to very sensitive imaging devices used for the successful detection of gravitational waves (Cao et al. 2020).

Our implementation of optical lock-in spectrometry is based in the following principles. The optical signal to analyze is split into two parallel channels using optical fibers. The first optical channel is modulated in-phase with a reference signal and the second optical channel is modulated in quadrature. The resulting modulated optical signals are sent to two identical array spectrometers. The low pass filtering stage is performed "physically" by the accumulation of electrical charges in each pixel during the integration time of the spectrometers. This principle allows lock-in detection to be performed simultaneously on every pixel of the array spectrometers within a few seconds. No signal processing is necessary to provide the resulting amplitude and phase spectra over the whole spectral range of the spectrometers.

3. Theory of optical lock-in spectrometry

When a light source exhibits temporal light modulation, its spectral radiant flux $S(t,\lambda)$ comprises a continuous (dc) component $S_{dc}(\lambda)$ and an alternative (ac) component $S_{ac}(t,\lambda)$. We assume here that both components depend on the wavelength. Like any periodic signal, the alternative component $S_{ac}(t,\lambda)$ can be expanded into a Fourier series. The expression of the spectral radiant flux is then written as follows:

$$S(t,\lambda) = S_{dc}(\lambda) + S_{ac}(t,\lambda) = S_{dc}(\lambda) + \sum_{n=1}^{\infty} S_n(\lambda)\cos\left(2\pi n f t - \varphi_n(\lambda)\right) \quad (1)$$

where *f* is the fundamental modulation frequency of the spectral radiant flux, $S_n(\lambda)$and $\varphi_n(\lambda)$ respectively are the amplitude and the phase of the Fourier component of the spectral radiant flux at frequency $n \times f$. The spectral quantities $S_n(\lambda)$ and $\varphi_n(\lambda)$ are the respective modulation amplitude spectrum and phase spectrum of the temporal light modulation at frequency $n \times f$. The phase value is a measure of the temporal lag of a given Fourier component of the spectral radiant flux at a given wavelength, with respect to an arbitrary point of the modulation cycle taken as an origin. The difference between phase values at two different wavelengths is related to the time difference between the corresponding components of the spectral radiant flux. The phase difference can carry useful information about the physical processes of optical emission involved in the light source.

Author's version of the following published article:
Martinsons C, Picard N, and Carré S. "Optical Lock-in Spectrometry Reveals Useful Spectral Features of Temporal Light Modulation in Several Light Source Technologies." *LEUKOS*, June 22, 2022, 1–19. https://doi.org/10.1080/15502724.2022.2077754.

The principle of optical lock-in spectrometry is to measure the spectral radiant flux using two identical spectrometers whose entrance ports are both amplitude-modulated at frequency *f*. The first spectrometer is modulated in phase and the second spectrometer is modulated in phase quadrature.

The transmission function at the entrance port of the in-phase spectrometer can be modeled by the following equation:

$$T_I(t) = \frac{1}{2}(\cos(2\pi f t) + 1) \tag{2}$$

Similarly, the transmission function at the entrance of quadrature spectrometer can be written as:

$$T_Q(t) = \frac{1}{2}(\sin(2\pi f t) + 1) \tag{3}$$

The resulting optical signal at the entrance of the in-phase spectrometer can be expressed as the product of the spectral radiant flux of the light source by the transmission function $T_I(t)$:

$$S_I(t,\lambda) = \frac{1}{2}(\cos(2\pi f t) + 1)\left(S_{dc}(\lambda) + \sum_{n=1}^{\infty} S_n(\lambda)\cos\left(2\pi n f t - \varphi_n(\lambda)\right)\right) \tag{4}$$

The development of the previous equation gives the following expression:

$$\begin{aligned} S_I(t,\lambda) = {} & \frac{1}{2}S_{dc}(\lambda) + \frac{1}{2}S_{dc}(\lambda)\cos(2\pi f t) + \frac{1}{2}\sum_{n=1}^{\infty} S_n(\lambda)\cos\left(2\pi n f t - \varphi_n(\lambda)\right) \\ & + \frac{1}{4}\sum_{n=1}^{\infty} S_n(\lambda)\left[\cos\left(2\pi(n+1)f t - \varphi_n(\lambda)\right) + \cos\left(2\pi(n-1)f t - \varphi_n(\lambda)\right)\right] \end{aligned} \tag{5}$$

If the integration time of the spectrometers is much greater than a modulation period, the charge accumulation in the pixels of the detector array acts as a low pass filter, giving the time-average value $\overline{S_I}(\lambda)$ of $S_I(t,\lambda)$. In Equation (5), only two terms have a non-zero time-average value: the first term and the last term with *n=1*. The output of the in-phase spectrometer is therefore:

Author's version of the following published article:
Martinsons C, Picard N, and Carré S. "Optical Lock-in Spectrometry Reveals Useful Spectral Features of Temporal Light Modulation in Several Light Source Technologies." *LEUKOS*, June 22, 2022, 1–19. https://doi.org/10.1080/15502724.2022.2077754.

$$\overline{S_I}(\lambda) = \frac{1}{2}S_{dc}(\lambda) + \frac{1}{4}S_1(\lambda)\cos\left(\varphi_1(\lambda)\right) \tag{6}$$

Following the same approach, the output of the quadrature spectrometer is given by a similar equation:

$$\overline{S_Q}(\lambda) = \frac{1}{2}S_{dc}(\lambda) + \frac{1}{4}S_1(\lambda)\sin\left(\varphi_1(\lambda)\right) \tag{7}$$

In order to eliminate the continuous component $S_{dc}(\lambda)$ from the spectrometer readings, a background subtraction can be performed on each spectrometer, with the optical modulator kept in a "half-open" configuration, while the light source under test is operating. Because of the quadrature setting of the modulator, the "half-open" configuration of a given channel corresponds either to the closed position or the open position of the other channel.

After this background subtraction step, the respective outputs of the spectrometers are given by the following equations:

$$I_1(\lambda) = \overline{S_I}(\lambda) - \frac{1}{2}S_{dc}(\lambda) \tag{8}$$

$$Q_1(\lambda) = \overline{S_Q}(\lambda) - \frac{1}{2}S_{dc}(\lambda) \tag{9}$$

Based on these expressions, equations (6) and (7) can be simplified to give the expressions of the amplitude and phase spectra:

$$S_1(\lambda) = 4\sqrt{I_1(\lambda)^2 + Q_1(\lambda)^2} \tag{10}$$

$$\varphi_1(\lambda) = \operatorname{atan}\left(\frac{Q_1(\lambda)}{I_1(\lambda)}\right) \tag{11}$$

Author's version of the following published article:
Martinsons C, Picard N, and Carré S. "Optical Lock-in Spectrometry Reveals Useful Spectral Features of Temporal Light Modulation in Several Light Source Technologies." *LEUKOS*, June 22, 2022, 1–19. https://doi.org/10.1080/15502724.2022.2077754.

The spectral modulation is defined as the ratio between the modulation amplitude spectrum and the dc component of the spectral radiant flux:

$$mod(\lambda) = \frac{S_1(\lambda)}{S_{dc}(\lambda)} \tag{12}$$

Unlike the standard modulation rate, the spectral modulation defined by Equation (12) can exceed 100% because the modulation amplitude is based on a Fourier component which can be greater than the total amplitude with certain types of non-sinusoidal waveforms (square waves for instance).

The phase is not mathematically defined when the modulation amplitude is null. Similarly, the spectral modulation is not defined when the spectral radiant flux is null. In practice, a significant amount of noise can be expected in the estimation of the phase and the spectral modulation when the spectral radiant flux and/or modulation amplitude approach their respective noise level.

4. Experimental setup

The optical lock-in spectrometry technique was implemented in the spectral radiant flux measurement facility of a photometry laboratory. The layout of the experimental setup is shown in

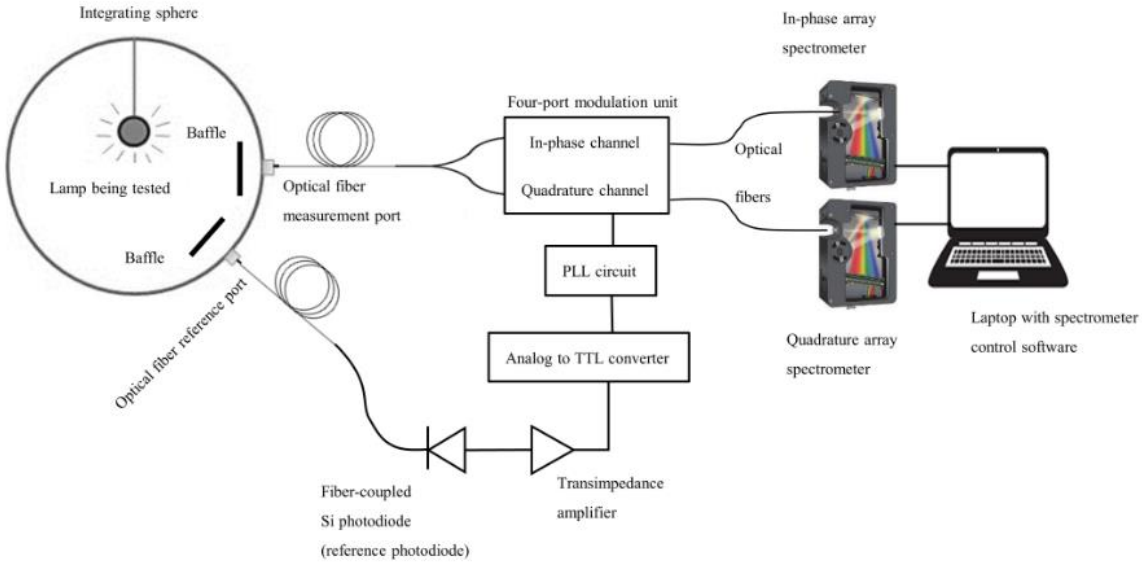

Figure 1. This facility is based on a 1 m diameter integrating sphere, fitted with two fiber optics ports. The reference port is connected to a silicon photodiode. A transimpedance amplifier provides the temporal light waveform of the light source under test. This analog signal is fed to a custom-made

Author's version of the following published article:
Martinsons C, Picard N, and Carré S. "Optical Lock-in Spectrometry Reveals Useful Spectral Features of Temporal Light Modulation in Several Light Source Technologies." *LEUKOS*, June 22, 2022, 1–19. https://doi.org/10.1080/15502724.2022.2077754.

analog to TTL converter designed to provide a reference signal to a PLL unit driving an optical modulator.

The analog to TTL converter is an electronic circuit based on a high pass filter to remove the dc component of the temporal light waveform, followed by a Schmitt trigger designed with an LM239 comparator chip. The output of this device is a square wave synchronized with the temporal waveform, as illustrated in

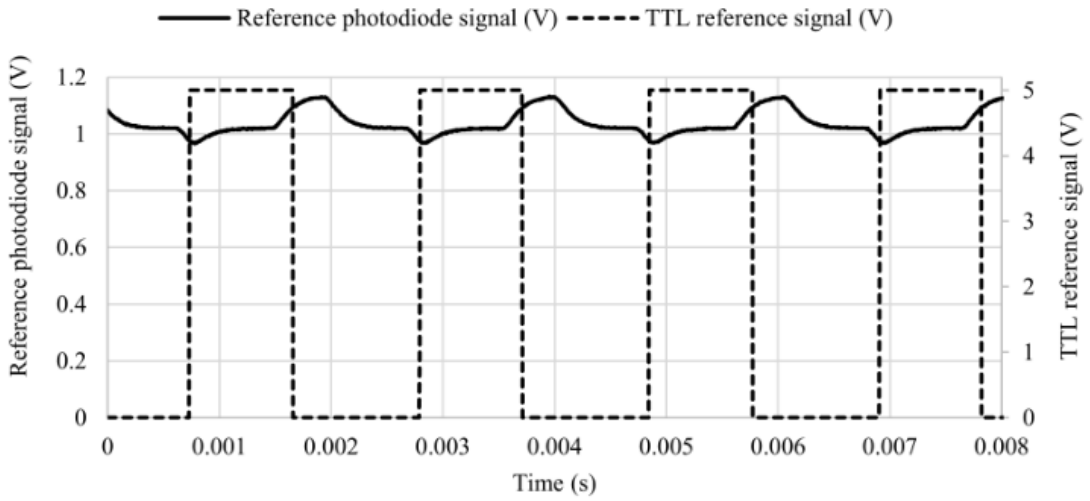

Figure 2. The TTL reference signal is then fed to a PLL unit. In our setup, the PLL unit is integrated in the controller of the modulation unit.

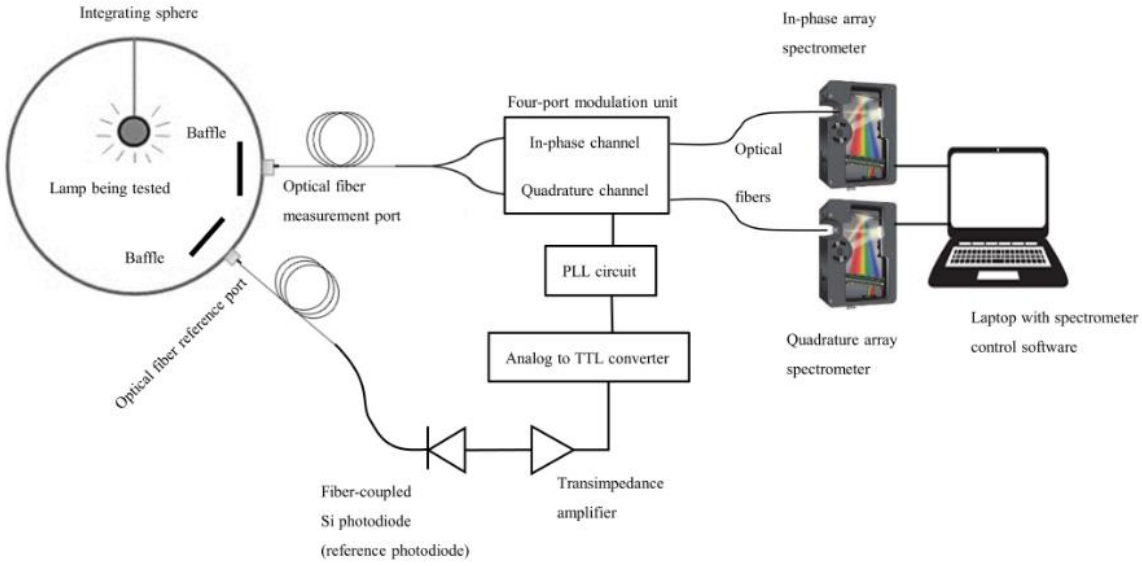

Figure 1. Schematic layout of the optical lock-in spectrometry setup

Author's version of the following published article:
Martinsons C, Picard N, and Carré S. "Optical Lock-in Spectrometry Reveals Useful Spectral Features of Temporal Light Modulation in Several Light Source Technologies." *LEUKOS*, June 22, 2022, 1–19. https://doi.org/10.1080/15502724.2022.2077754.

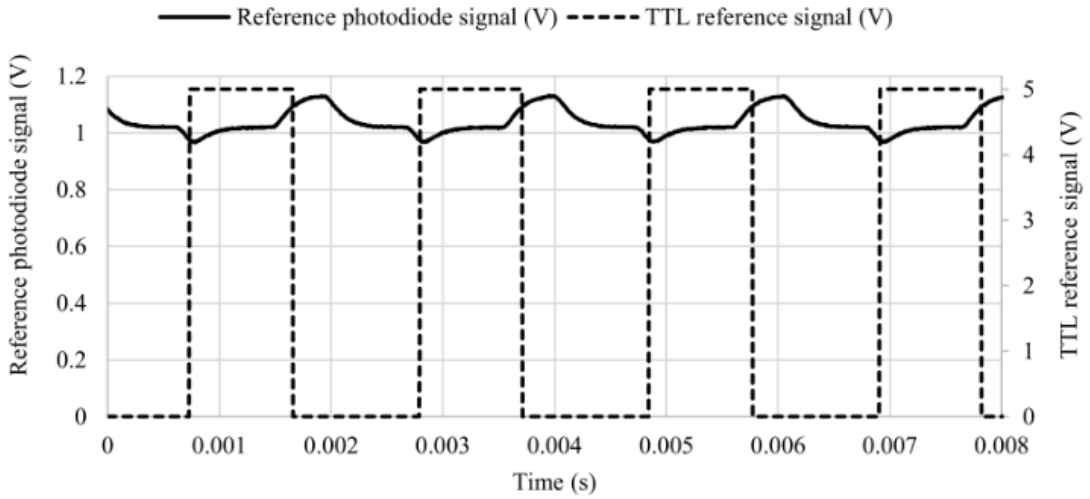

Figure 2. Graph showing a temporal light waveform (solid line) and the synchronized signal generated by the analog to TTL converter of the experimental setup (dashed line).

The measurement port of the integrating sphere is connected to a Y-bifurcated optical fiber used to split the optical signal in two equal parts. The two resulting identical signals are sent to an optical modulation unit. The unit is based on a rotary optical chopper and four optical ports each consisting in a fiber-optics 90° off-axis parabolic collimator. The unit was designed to produce well collimated beams with a diameter comparable to the size of the chopper blade openings. The collimators were placed in quadrature arrangement: when one channel is open or closed by the blade, the other channel is half-open. A schematic view of the modulation unit is shown in

Author's version of the following published article:
Martinsons C, Picard N, and Carré S. "Optical Lock-in Spectrometry Reveals Useful Spectral Features of Temporal Light Modulation in Several Light Source Technologies." *LEUKOS*, June 22, 2022, 1–19. https://doi.org/10.1080/15502724.2022.2077754.

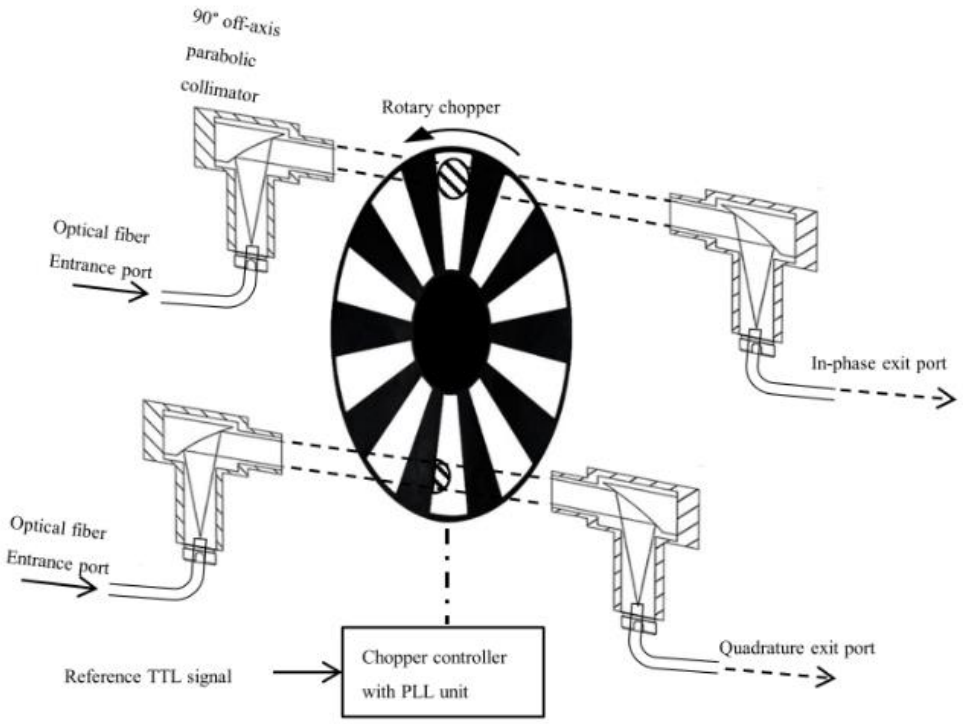

Figure 3. The resulting transmission functions were measured using photodiodes. The measured waveforms are close to pure sine and cosine waves (

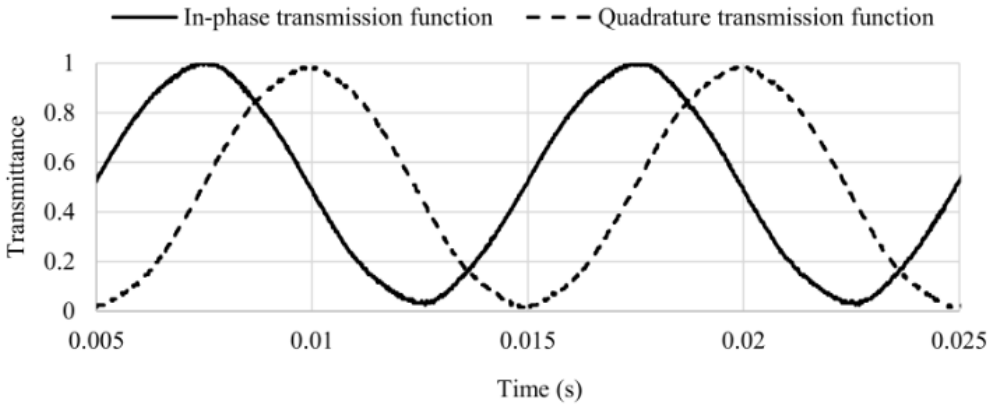

Figure 4). The maximum modulation frequency of this modulation unit is about 1000 Hz.

Author's version of the following published article:
Martinsons C, Picard N, and Carré S. "Optical Lock-in Spectrometry Reveals Useful Spectral Features of Temporal Light Modulation in Several Light Source Technologies." *LEUKOS*, June 22, 2022, 1–19. https://doi.org/10.1080/15502724.2022.2077754.

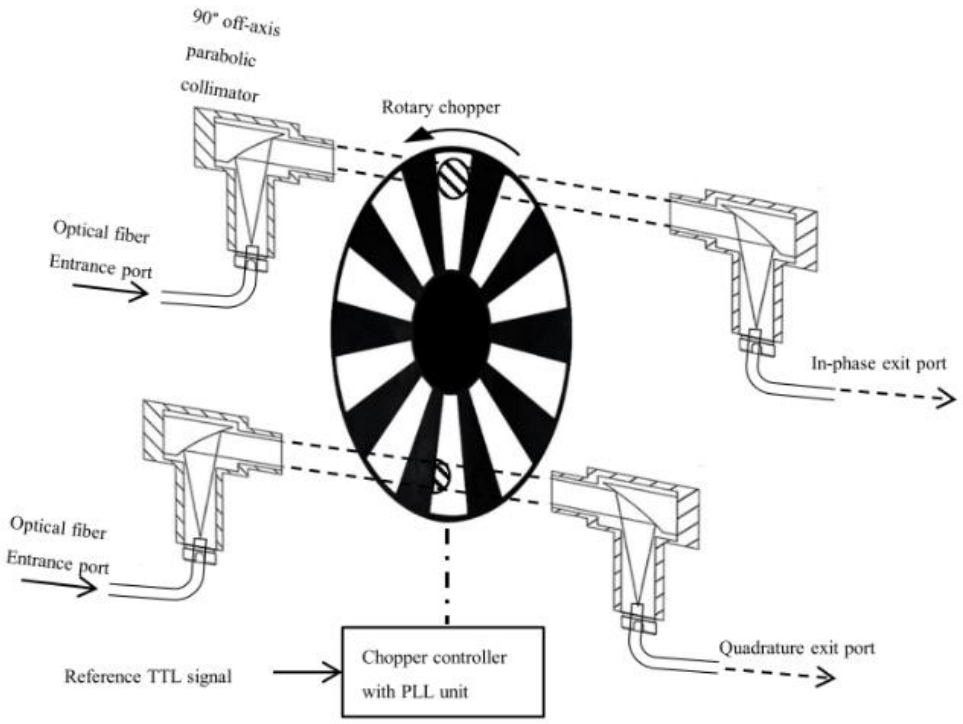

Figure 3. Schematic layout of the four-port modulation unit

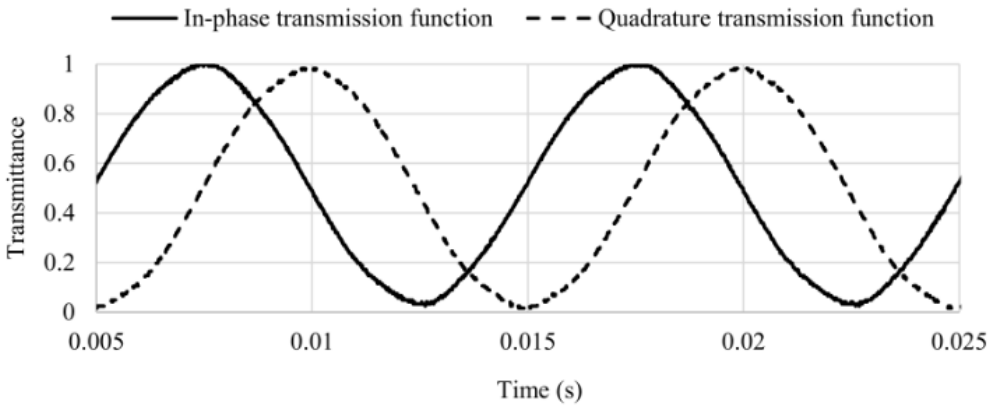

Figure 4. Measured transmission functions of the four-port modulation unit

The outputs of the modulation unit are connected with optical fibers to the entrance ports of two identical compact array spectrometers. The absolute calibration of the two spectrometers was carried out using a calibrated spectral radiant flux standard lamp traceable to NIST standards. The standard lamp was installed in the integrating sphere during the calibration. Each spectrometer was

Author's version of the following published article:
Martinsons C, Picard N, and Carré S. "Optical Lock-in Spectrometry Reveals Useful Spectral Features of Temporal Light Modulation in Several Light Source Technologies." *LEUKOS*, June 22, 2022, 1–19. https://doi.org/10.1080/15502724.2022.2077754.

calibrated with the modulation unit set in the "open" configuration for their respective channel. During the calibration of the spectrometers, their respective readings were adjusted to the reference spectral radiant flux of the standard lamp. The calibration of the spectrometers was done using the same integration time (1 s) than the one used in the optical lock-in mode.

The spectrometers are controlled in real-time by the software provided by their manufacturer. The calibration, background subtraction and lock-in data acquisition were programmed and automated with the graphical interface of the manufacturer software.

5. Results

The optical lock-in spectrometry setup was applied to several types of lamps used in general lighting, including legacy technologies (now obsolete) and contemporary technologies based on LEDs. Table 1 provides the description of the tested lamps together with the measured CCT and color-rendering index Ra, as measured in the classical operating mode of the spectral radiant flux facility. The temporal light waveforms were measured using a V(λ)-corrected photometer. The measured temporal light waveforms are shown in

Author's version of the following published article:
Martinsons C, Picard N, and Carré S. "Optical Lock-in Spectrometry Reveals Useful Spectral Features of Temporal Light Modulation in Several Light Source Technologies." *LEUKOS*, June 22, 2022, 1–19. https://doi.org/10.1080/15502724.2022.2077754.

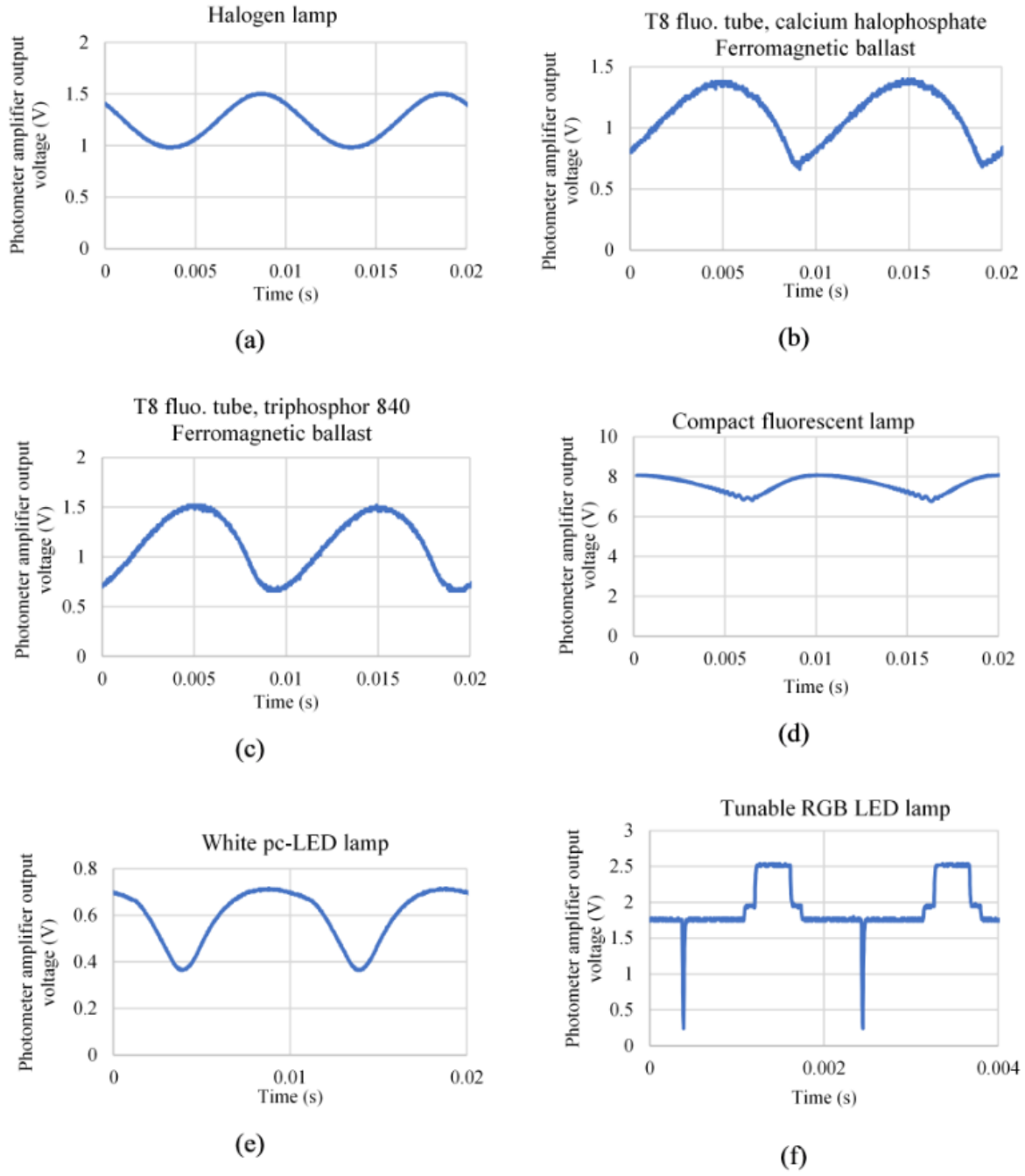

Figure 5. The latest CIE guidelines (CIE 2021) were applied to determine the standard temporal light modulation metrics: short-term visibility flicker index (PstLM), stroboscopic visibility measure (SVM), modulation percent (mod%) and dominant modulation frequency. All the tested lamps were powered using a stable laboratory power supply set at 230 V and 50 Hz. The lamps were operated for at least 20 minutes before being tested. The settings of the two array spectrometers that were used for lock-in measurements are detailed in Table 2.

Author's version of the following published article:
Martinsons C, Picard N, and Carré S. "Optical Lock-in Spectrometry Reveals Useful Spectral Features of Temporal Light Modulation in Several Light Source Technologies." *LEUKOS*, June 22, 2022, 1–19. https://doi.org/10.1080/15502724.2022.2077754.

Table 1. Characteristics of the tested lamps

Lamp	Model	CCT	Ra	PstLM	SVM	Mod%	Mod. Freq.
Incandescent lamp tungsten-halogen	Philips Ecoclassic 28W	2694 K	99	0.066	0.794	21.2%	100 Hz
Fluorescent tube (*) T8 calcium halophosphate ferromagnetic ballast	Mazda Fluor Blanc Industrie 33 TF 18 W (vintage unit from 1992)	4228 K	63	0.219	1.018	33.8%	100 Hz
Fluorescent tube T8 Tri-phosphor 840 ferromagnetic ballast	Philips MASTER TL-D 18 W	3949 K	81	0.215	1.396	39.2%	100 Hz
Compact fluorescent lamp high frequency integrated ballast	Philips Tornado 15W	6485 K	82	0.019	0.261	8.3%	100 Hz
White LED lamp Chip-on-board type	Philips 8 W E27	2742 K	84	0.108	1.300	34.7%	100 Hz
Tunable RGB LED lamp Chosen color setting: R=51 G=255 B=81	Smart Light Avanquest 7.5W	-	-	0.06	0.287	82.7%	486 Hz

(*) Note: the halophosphate fluorescent tube is largely obsolete. It was tested for the purpose of comparing the spectral modulation measurements with data published in (Wilkins and Clark 1990).

Table 2. Settings of the array spectrometers

Setting	Value
Width of entrance slit	5 µm
Grating	600 lines per mm blazed at 300 nm
Wavelength range of interest	380 nm to 780 nm
Average optical resolution	0.99 nm
Integration time	1 s
Number of averages	4
Boxcar averages	1 for fluorescent lamps 2 for other lamps

Author's version of the following published article:
Martinsons C, Picard N, and Carré S. "Optical Lock-in Spectrometry Reveals Useful Spectral Features of Temporal Light Modulation in Several Light Source Technologies." *LEUKOS*, June 22, 2022, 1–19. https://doi.org/10.1080/15502724.2022.2077754.

Wavelength interpolation step of spectral output data	0.1 nm for fluorescent lamps 1 nm for other lamps

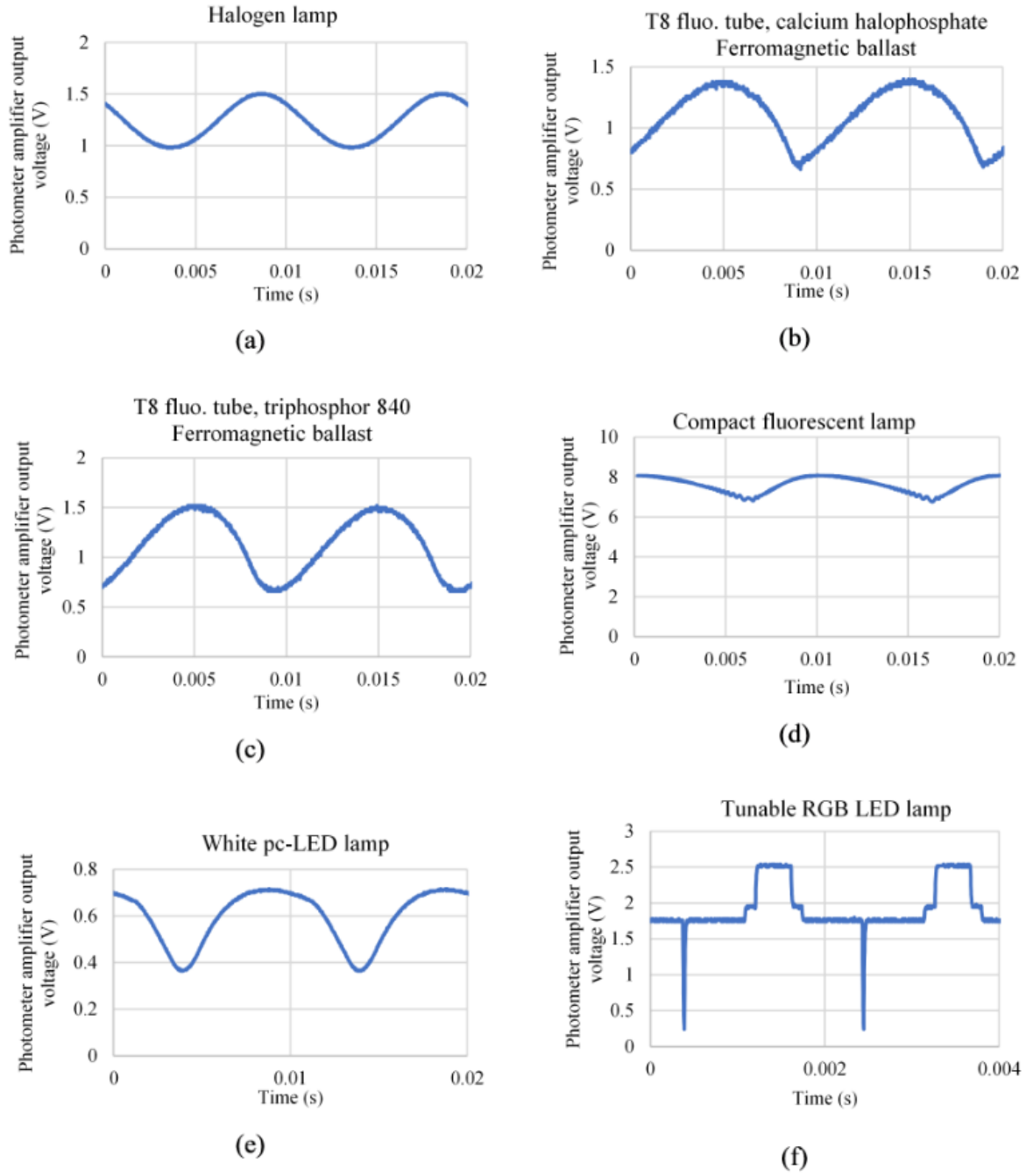

Figure 5. (a) to (f) : Temporal light modulation waveforms of the tested lamps

5.1. Incandescent lamp

Author's version of the following published article:
Martinsons C, Picard N, and Carré S. "Optical Lock-in Spectrometry Reveals Useful Spectral Features of Temporal Light Modulation in Several Light Source Technologies." *LEUKOS*, June 22, 2022, 1–19. https://doi.org/10.1080/15502724.2022.2077754.

A low wattage tungsten-halogen lamp was chosen because of its relatively high level of temporal light modulation, resulting from a thin filament with low thermal inertia. The results of the lock-in measurements are shown in

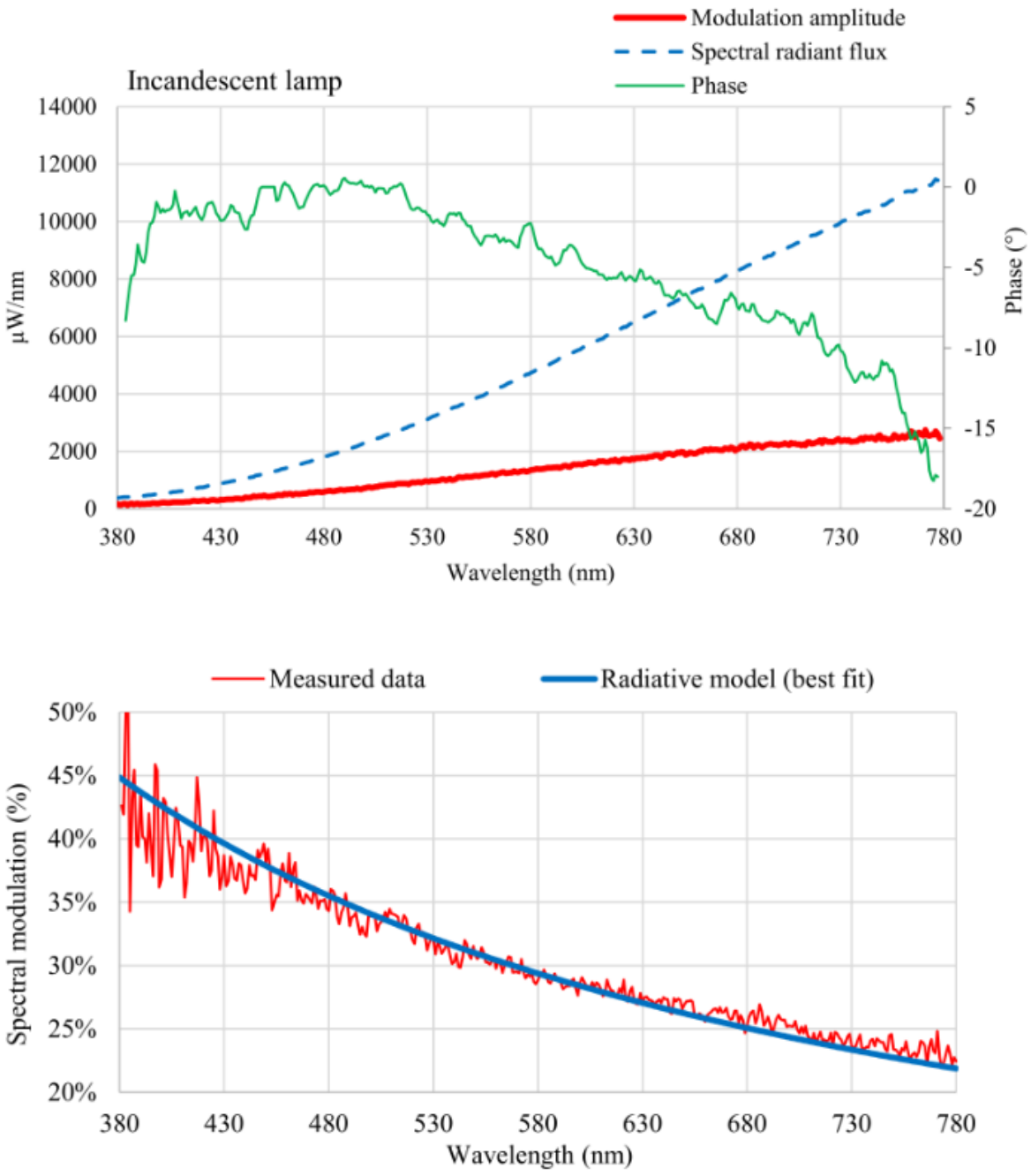

Figure 6.

Author's version of the following published article:
Martinsons C, Picard N, and Carré S. "Optical Lock-in Spectrometry Reveals Useful Spectral Features of Temporal Light Modulation in Several Light Source Technologies." *LEUKOS*, June 22, 2022, 1–19. https://doi.org/10.1080/15502724.2022.2077754.

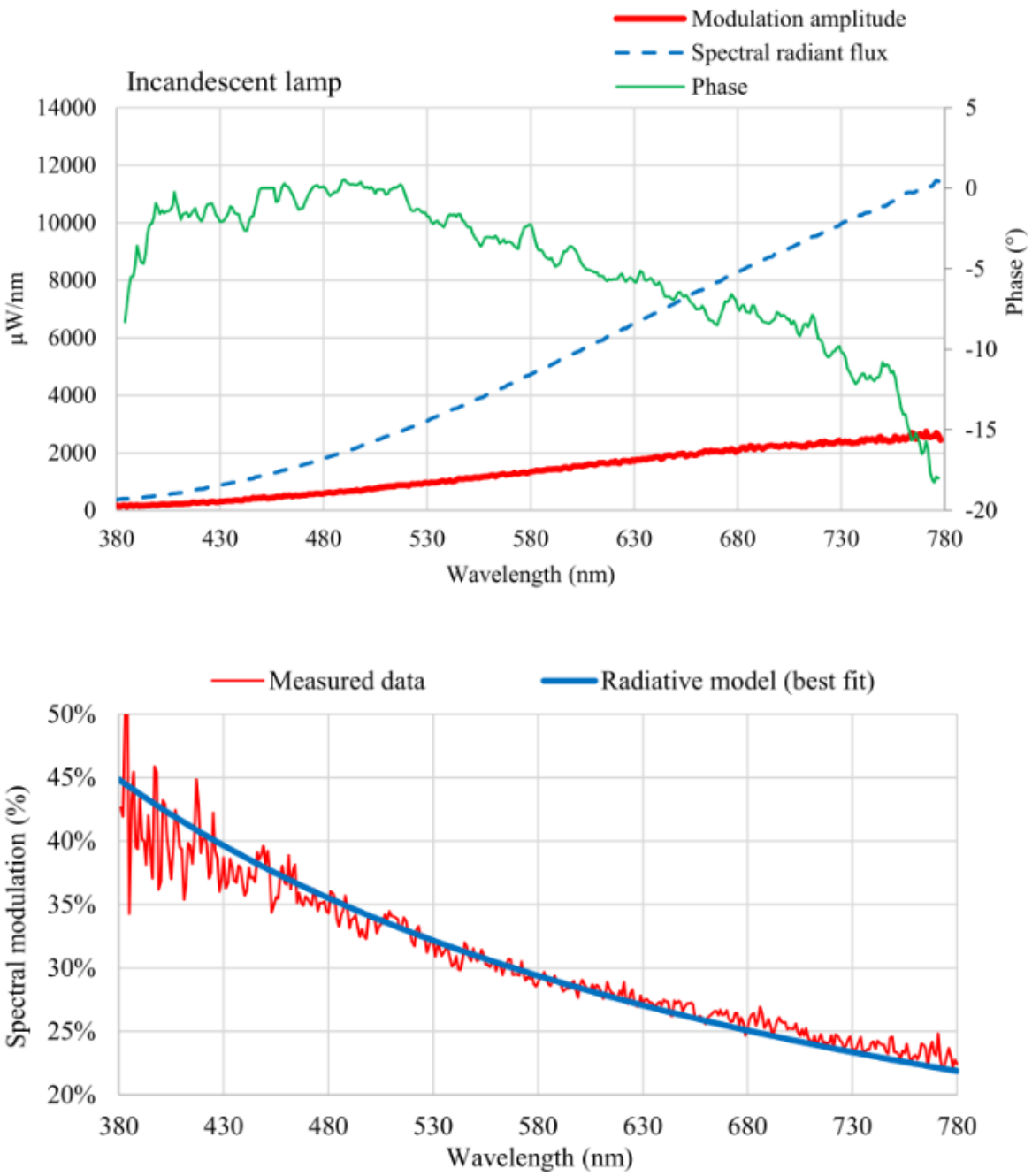

Figure 6. The upper graph shows the spectral radiant flux (dashed line), the amplitude (red solid line) and phase (green solid line) spectra of the tested halogen lamp. The bottom graph shows the measured spectral modulation and the best fit obtained with the model derived from Planck's formula.

The spectral modulation decreases with the wavelength, approximately following a $1/\lambda$ relationship. The spectral modulation is about 43% at 380 nm and about 23% at 780 nm. The spectral modulation data are noisy below 430 nm because the level of blue light emitted by the lamp is low and the noise level in the spectral radiant flux data becomes critical in the division made according to Equation (12).

Author's version of the following published article:
Martinsons C, Picard N, and Carré S. "Optical Lock-in Spectrometry Reveals Useful Spectral Features of Temporal Light Modulation in Several Light Source Technologies." *LEUKOS*, June 22, 2022, 1–19. https://doi.org/10.1080/15502724.2022.2077754.

This observed variation in spectral modulation can be explained by considering the blackbody radiation of the lamp filament in a thermal modulated regime. Assuming that the filament is a blackbody at absolute temperature T undergoing a small periodic temperature oscillation of amplitude T_{ac}, the spectral modulation can be approximated by the following equation:

$$mod(\lambda) = \frac{1}{L_\lambda}\left(\frac{\partial L_\lambda}{\partial T}\right)T_{ac} \tag{13}$$

where L_λ is the Planck's spectral radiance. Using Planck's formula, Equation (13) becomes:

$$mod(\lambda) \cong \frac{c_2}{\lambda T^2}T_{ac} \tag{14}$$

Author's version of the following published article:
Martinsons C, Picard N, and Carré S. "Optical Lock-in Spectrometry Reveals Useful Spectral Features of Temporal Light Modulation in Several Light Source Technologies." *LEUKOS*, June 22, 2022, 1–19. https://doi.org/10.1080/15502724.2022.2077754.

where c_2 is the second radiation constant (Hartmann 2006). Equation (14) was used to fit the spectral modulation data. The best fit, shown in the bottom graph of

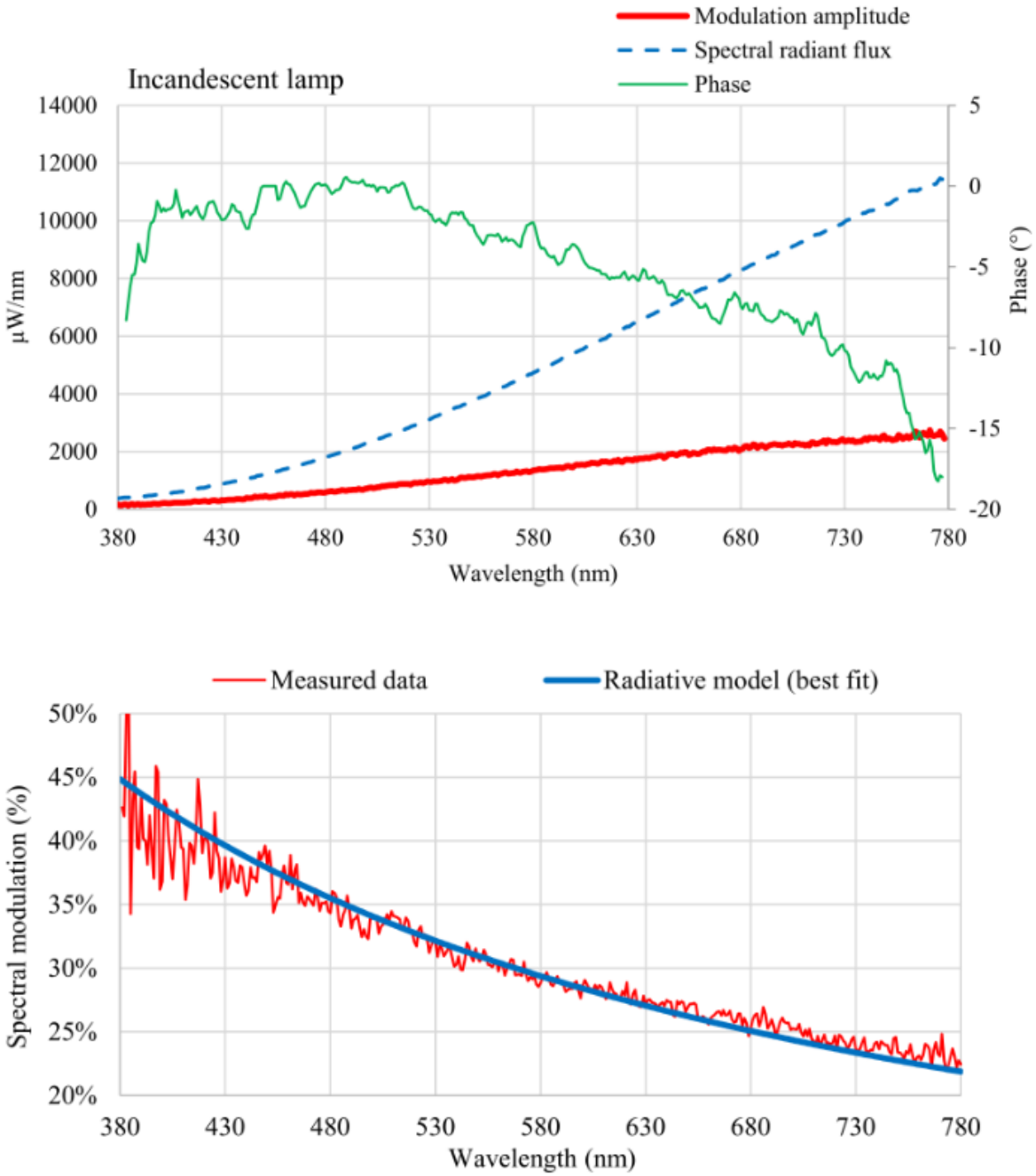

Figure 6, was obtained with T = 2694 K (the measured correlated color temperature of this lamp) and T_{ac} = 86 K. Although the fit shows a small residual deviation, the spectral modulation data are in good agreement with this simple model.

Author's version of the following published article:
Martinsons C, Picard N, and Carré S. "Optical Lock-in Spectrometry Reveals Useful Spectral Features of Temporal Light Modulation in Several Light Source Technologies." *LEUKOS*, June 22, 2022, 1–19. https://doi.org/10.1080/15502724.2022.2077754.

The phase spectrum is not monotonous. The phase lag is minimal in the blue-green part of the spectrum around 480 nm. The phase lag regularly increases towards the red and blue ends of the spectrum. This spectral behavior has not been investigated in this work.

5.2. Fluorescent lamps

Three types of fluorescent lamps have been studied: a halophosphate fluorescent tube, a tri-phosphor fluorescent tube and a compact fluorescent lamp (CFL).

5.2.1.Halophosphate fluorescent tube with ferromagnetic ballast

Halophosphate fluorescent tubes were used from the 1950s until they were completely replaced during the 1980s and the 1990s by tri-phosphor fluorescent tubes having much better color-rendering properties (DiLaura et al. 2011). A halophosphate T8 fluorescent tube dating from 1992 - in perfect condition - was tested to compare the results of optical lock-in spectrometry with measurement data published in 1990 by Wilkins and Clark (Wilkins and Clark 1990). The lamp was tested with a ferromagnetic ballast, as reported in the original paper.

The spectral radiant flux and modulation amplitude spectrum are shown in

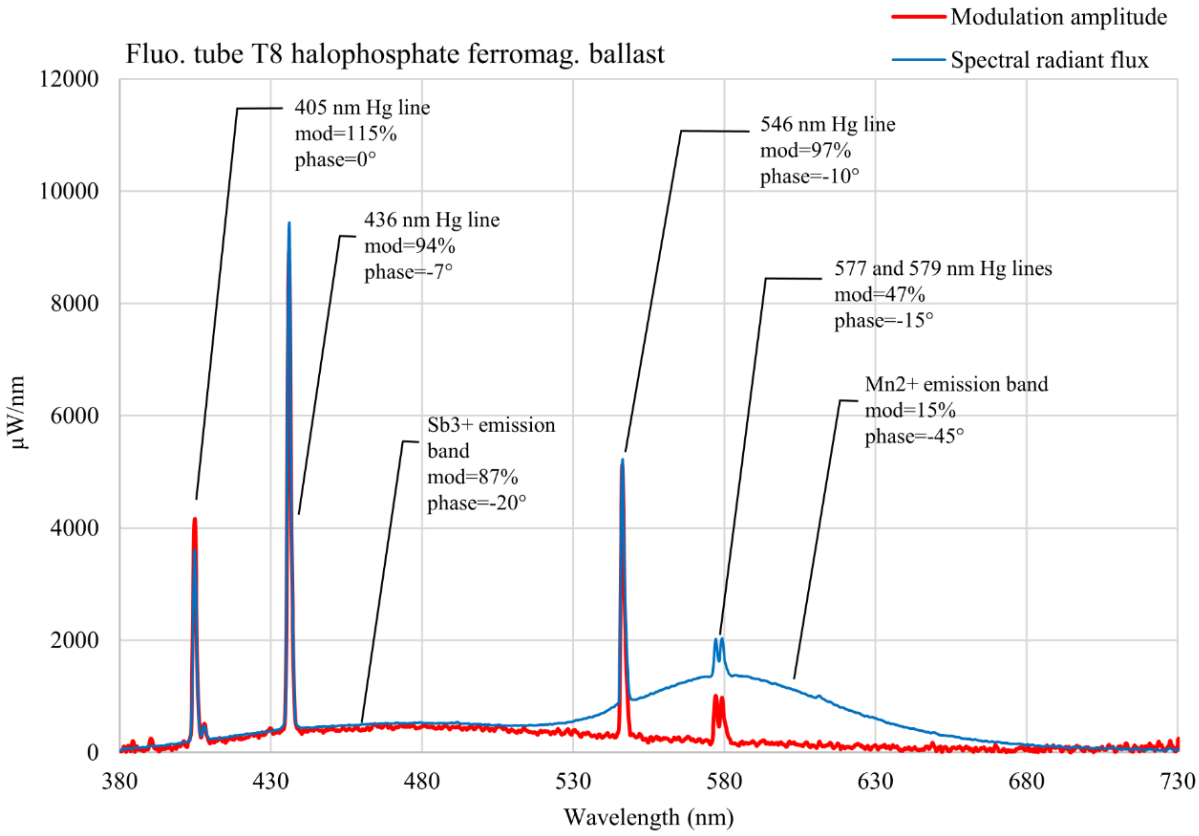

Figure 7. Five emissions mercury lines are detected in the emission spectrum, superimposed to two

Author's version of the following published article:
Martinsons C, Picard N, and Carré S. "Optical Lock-in Spectrometry Reveals Useful Spectral Features of Temporal Light Modulation in Several Light Source Technologies." *LEUKOS*, June 22, 2022, 1–19. https://doi.org/10.1080/15502724.2022.2077754.

large emission bands in the blue-green and the orange-red spectral range, respectively corresponding to the emission of the antimony (Sb^{3+}) and the manganese (Mn^{2+}) luminophores of the calcium halophosphate (DiLaura et al. 2011). The amplitude spectrum below 500 nm is practically identical to the spectral radiant flux, meaning that the spectral modulation is very high in this spectral range. Above 500 nm, the modulation amplitude significantly decreases. This result shows that the manganese luminophore has a longer fluorescence lifetime compared with the antimony luminophore.

The spectral modulation and phase values are reported in

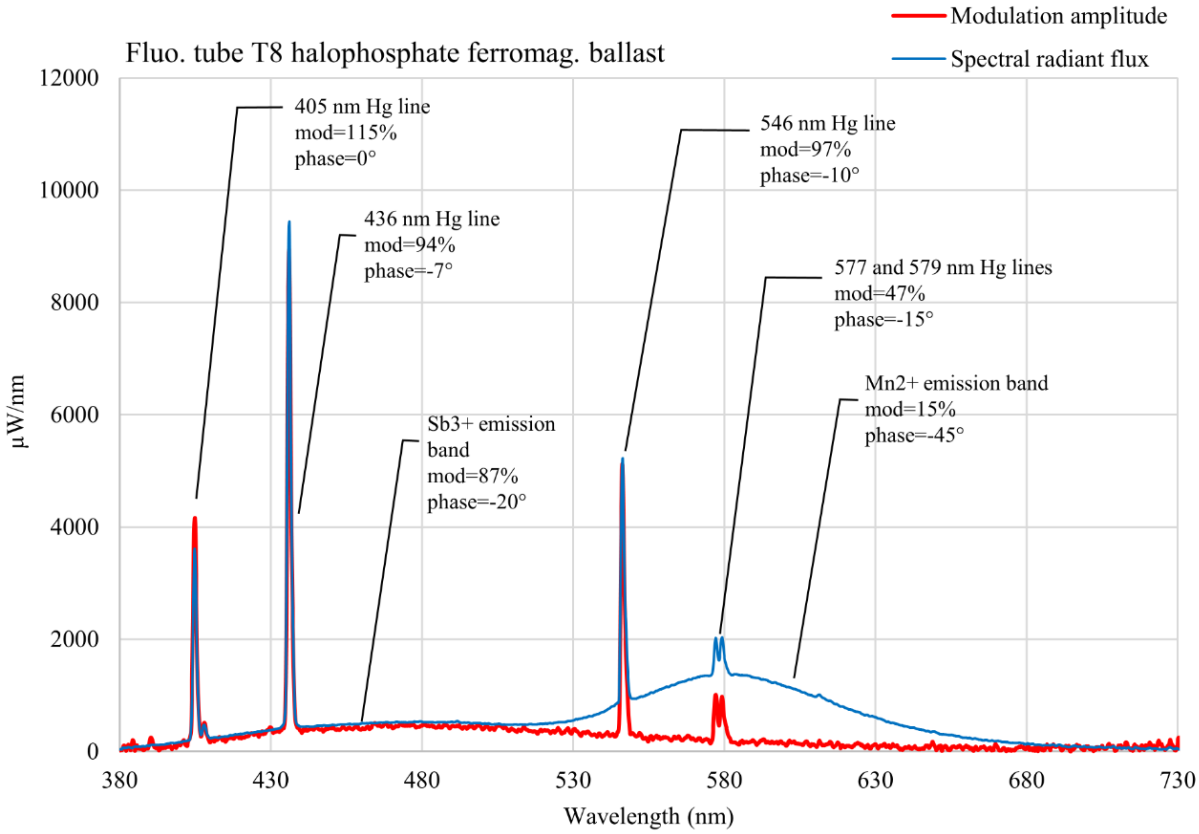

Figure 7 for each specific emission band. Outside the emission bands, the spectral modulation and phase data are very noisy because their calculation involves a ratio with a small quantity in the denominator.

The amplitude and phase of the modulated emission of a specific luminophore can be used to determine its fluorescence lifetime. If a single exponential decay is assumed for the temporal relaxation of a luminophore, its fluorescence lifetime τ can be determined from the following equations, used to measure fluorescence lifetimes in frequency-domain fluorometry (Vetromile and Jameson 2014):

Author's version of the following published article:
Martinsons C, Picard N, and Carré S. "Optical Lock-in Spectrometry Reveals Useful Spectral Features of Temporal Light Modulation in Several Light Source Technologies." *LEUKOS*, June 22, 2022, 1–19. https://doi.org/10.1080/15502724.2022.2077754.

$$\tan\left(\varphi_1(\lambda)\right) = 2\pi f\tau \tag{15}$$

$$mod(\lambda) = \frac{1}{\sqrt{1+(2\pi f\tau)^2}} \tag{16}$$

Using equations (15) and (16), the fluorescence lifetimes of the Sb^{3+} and the Mn^{2+} luminophores can be roughly estimated. The values are reported in Table 3. The lifetimes respectively estimated from the phase and the modulation data are in good agreement for Sb3+ but not in the case of Mn^{2+}. This is probably because the origin of the phase values is not known. In this measurement, the phase origin was arbitrarily adjusted to the 405 nm Hg emission line.

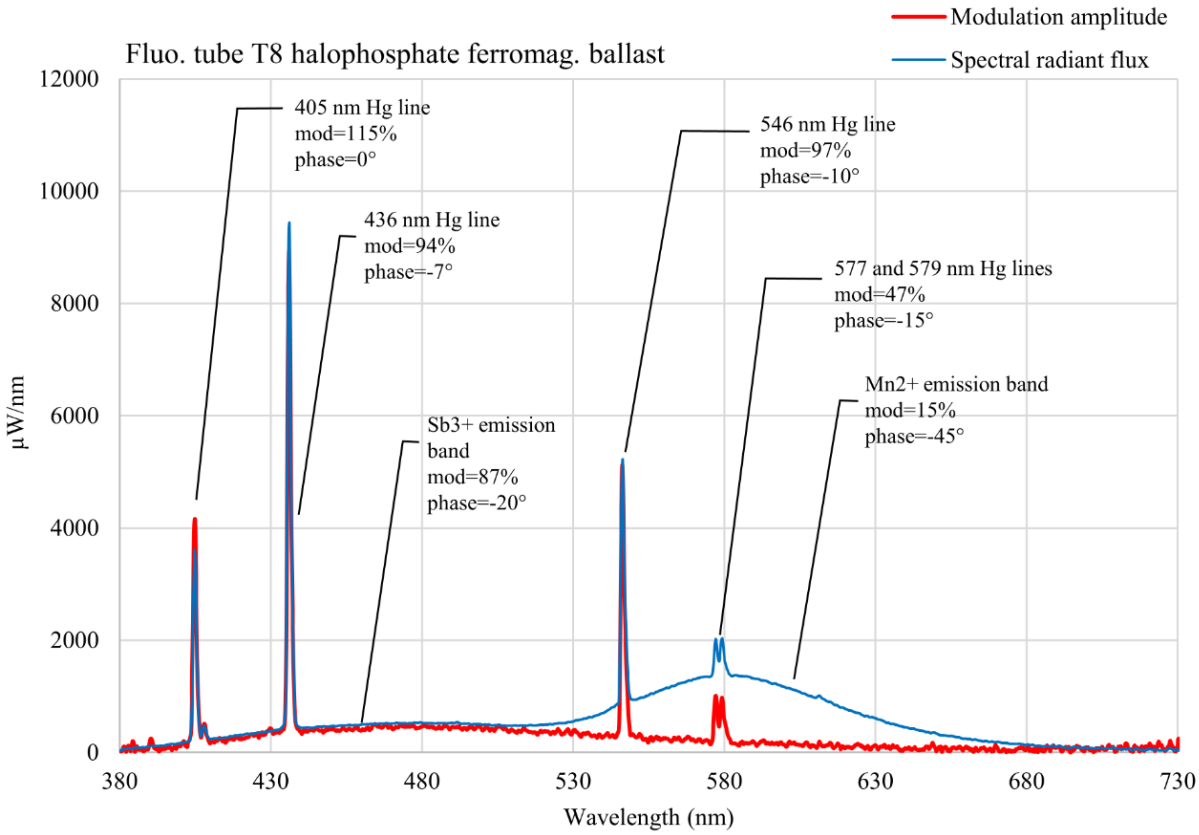

Figure 7. Spectral radiant flux (blue solid line) and modulation amplitude spectrum (red solid line) of the halophosphate fluorescent tube. The spectral modulation and phase values are reported for each specific emission band.

5.2.2.Tri-phosphor fluorescent tube with ferromagnetic ballast

Author's version of the following published article:
Martinsons C, Picard N, and Carré S. "Optical Lock-in Spectrometry Reveals Useful Spectral Features of Temporal Light Modulation in Several Light Source Technologies." *LEUKOS*, June 22, 2022, 1–19. https://doi.org/10.1080/15502724.2022.2077754.

Tri-phosphor fluorescent lamps were - and still are - a very common light source for the lighting of workplaces before the advent of solid-state lighting. In this lighting technology, three luminophores based on rare-earth dopants are used. A T8 tri-phosphor fluorescent tube (type 840) was tested with a ferromagnetic ballast to compare the results with data published in (Wilkins and Clark 1990).

The spectral radiant flux and modulation amplitude spectrum measured by optical lock-in spectrometry are shown in

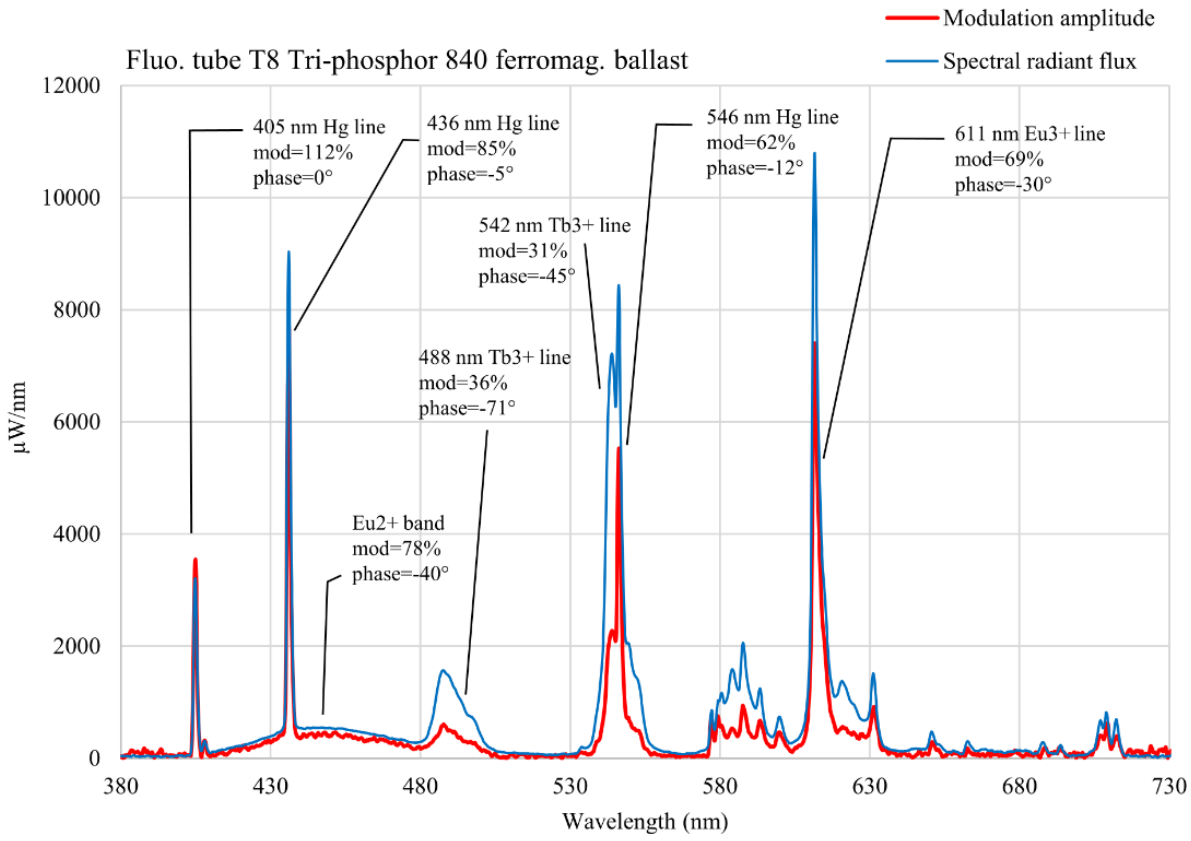

Figure 8. The spectral modulation and phase values are also reported in

Author's version of the following published article:
Martinsons C, Picard N, and Carré S. "Optical Lock-in Spectrometry Reveals Useful Spectral Features of Temporal Light Modulation in Several Light Source Technologies." *LEUKOS*, June 22, 2022, 1–19. https://doi.org/10.1080/15502724.2022.2077754.

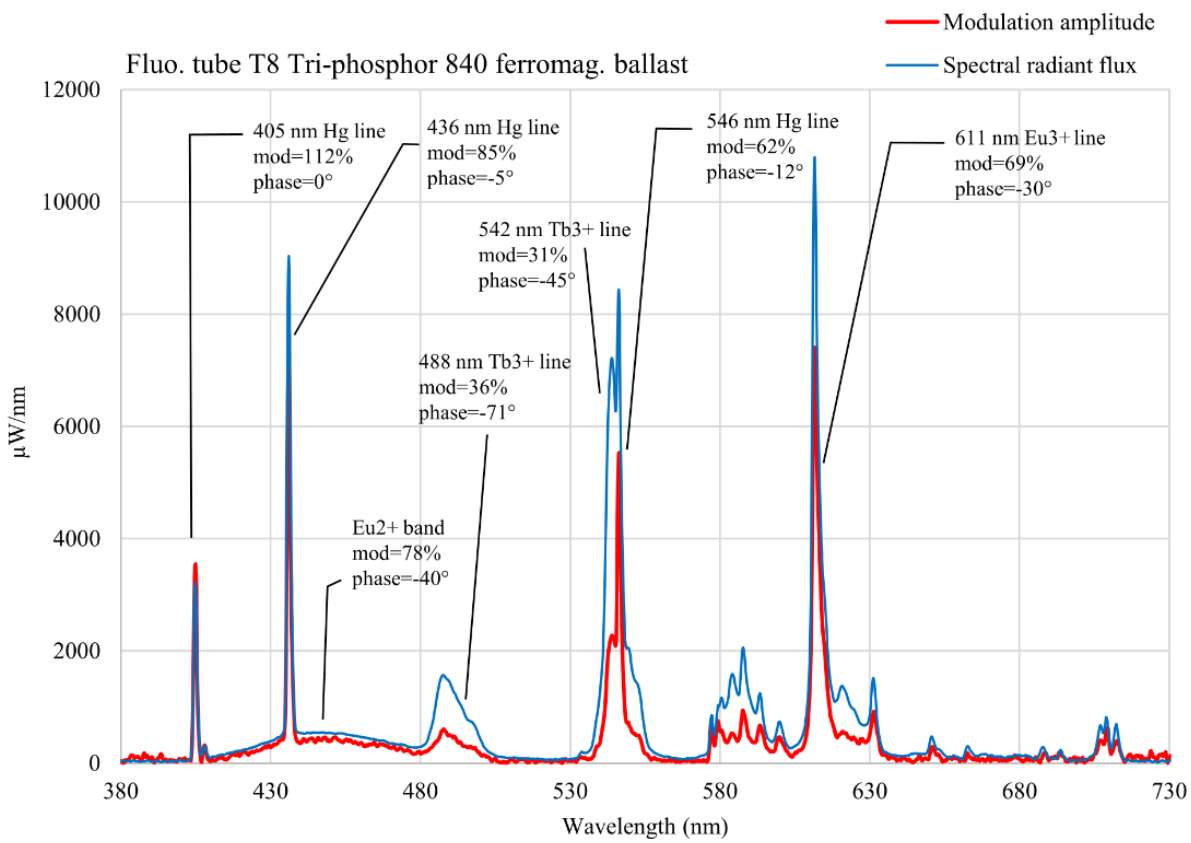

Figure 8 for the main emission lines.

Three intense emissions mercury lines are detected in the emission spectrum, as well as the blue broad band emission of the europium luminophore Eu^{2+}, the green emission band of the terbium luminophore Tb^{3+} and the emission line of europium Eu^{3+} in the red. Several other smaller lines are present in the orange and red parts of the spectrum.

The mercury lines show the highest modulation amplitudes, starting from 112% at 405 nm down to 62% at 546 nm. The Tb^{3+} emission bands are associated with the lowest spectral modulation (31% and 36%) and highest phase lags with respect to the 405 nm Hg line. The Eu^{3+} emission band at 611 nm has a spectral modulation of 69%.

Author's version of the following published article:
Martinsons C, Picard N, and Carré S. "Optical Lock-in Spectrometry Reveals Useful Spectral Features of Temporal Light Modulation in Several Light Source Technologies." *LEUKOS*, June 22, 2022, 1–19. https://doi.org/10.1080/15502724.2022.2077754.

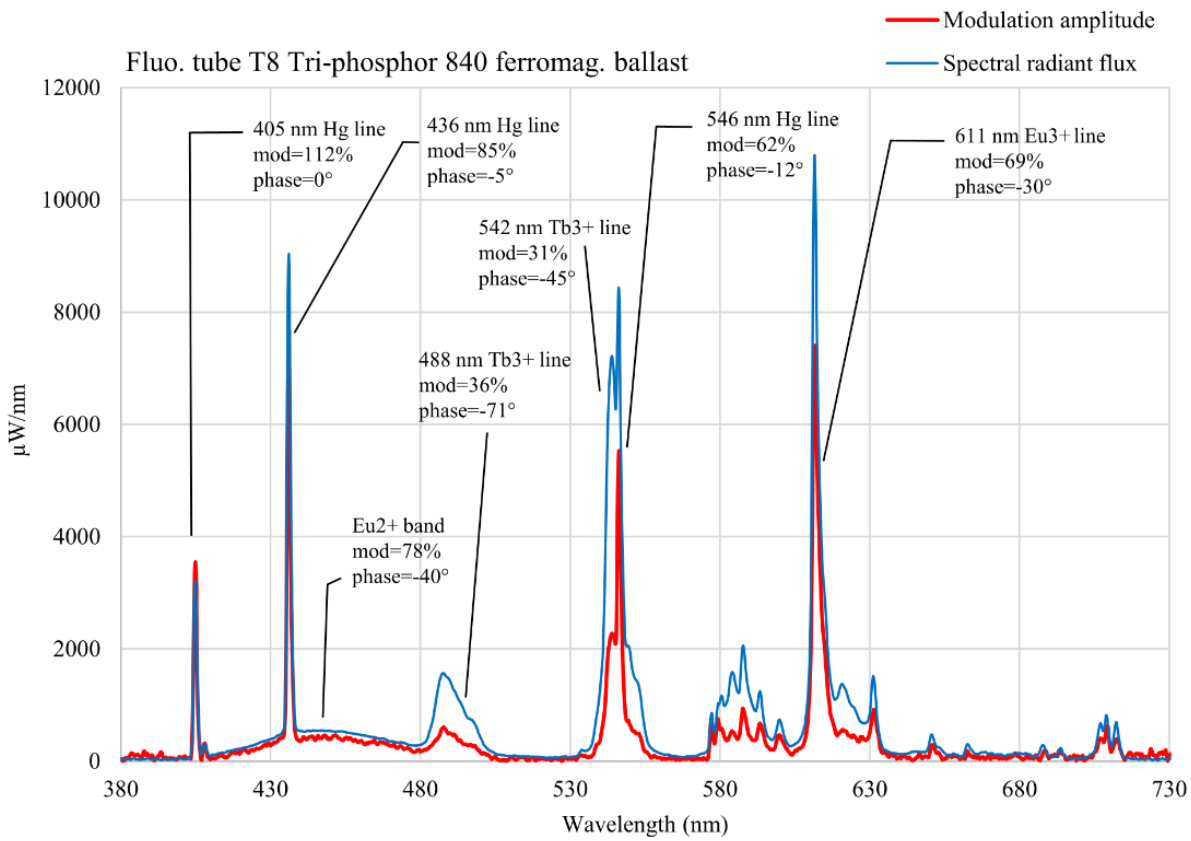

Figure 8. Spectral radiant flux (blue solid line) and modulation amplitude spectrum (red solid line) of the tri-phosphor fluorescent tube. The spectral modulation and phase values are reported for the main emission lines.

The fluorescence lifetimes of the three main luminophores were calculated using Equations (15) and (16). The results are reported in Table 3. Using both phase and modulation measurements, two consistent estimates of the Eu^{3+} luminophore are obtained. The lifetime estimations of Tb^{3+} and Eu^{2+} respectively calculated from the phase and modulation values show some discrepancies that could be attributed to the arbitrary setting of the origin of phase values on the 405 nm Hg line.

Table 3. Estimation of the fluorescence lifetime of the main luminophores in the tested fluorescent tubes

Author's version of the following published article:
Martinsons C, Picard N, and Carré S. "Optical Lock-in Spectrometry Reveals Useful Spectral Features of Temporal Light Modulation in Several Light Source Technologies." *LEUKOS*, June 22, 2022, 1–19. https://doi.org/10.1080/15502724.2022.2077754.

Lamp	Lumino-phore	Spectral band of interest	Estimated fluorescence lifetime from phase value	Estimated fluorescence lifetime from modulation value
Halophosphate tube	Sb^{3+}	380 – 500 nm	0.6 ms	0.6 ms
	Mn^{2+}	530 – 680 nm	1.6 ms	3.8 ms
Tri-phosphor tube	Eu^{2+}	415 - 475 nm	1.4 ms	0.8 ms
	Tb^{3+}	488 nm	4.6 ms	2.1 ms
		512 nm	1.6 ms	2.4 ms
	Eu^{3+}	611 nm	0.9 ms	1.1 ms

5.2.3.Comparison with data from Wilkins and Clark

Wilkins and Clark (Wilkins and Clark 1990) measured the spectral modulation of fluorescent lamps using a grating monochromator with a silicon photodiode placed against the exit slit. Their estimation of the spectral modulation was based on the temporal light waveform recorded by the photodiode at each wavelength with a spectral resolution of 5 nm. The measured temporal light waveforms were not purely sinusoidal. Therefore, the spectral modulation data were not related to a single frequency component - as it is the case in lock-in measurements - but included all frequency components. This is the reason why we expect our spectral modulation values to be slightly different.

Author's version of the following published article:
Martinsons C, Picard N, and Carré S. "Optical Lock-in Spectrometry Reveals Useful Spectral Features of Temporal Light Modulation in Several Light Source Technologies." *LEUKOS*, June 22, 2022, 1–19. https://doi.org/10.1080/15502724.2022.2077754.

in

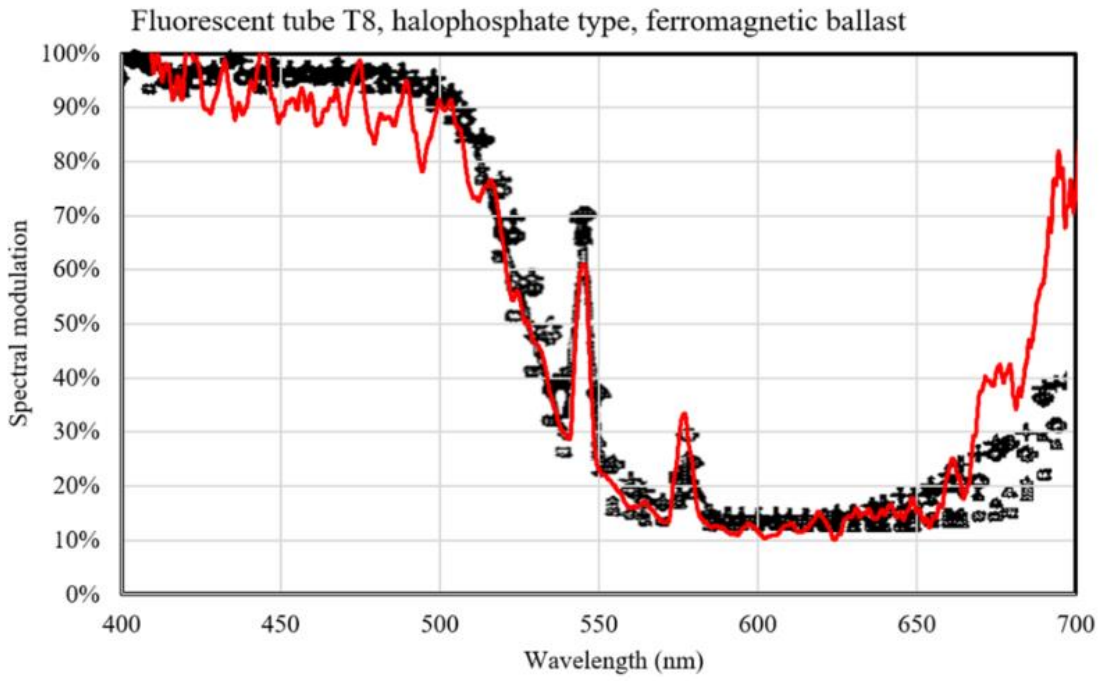

Figure 9 and

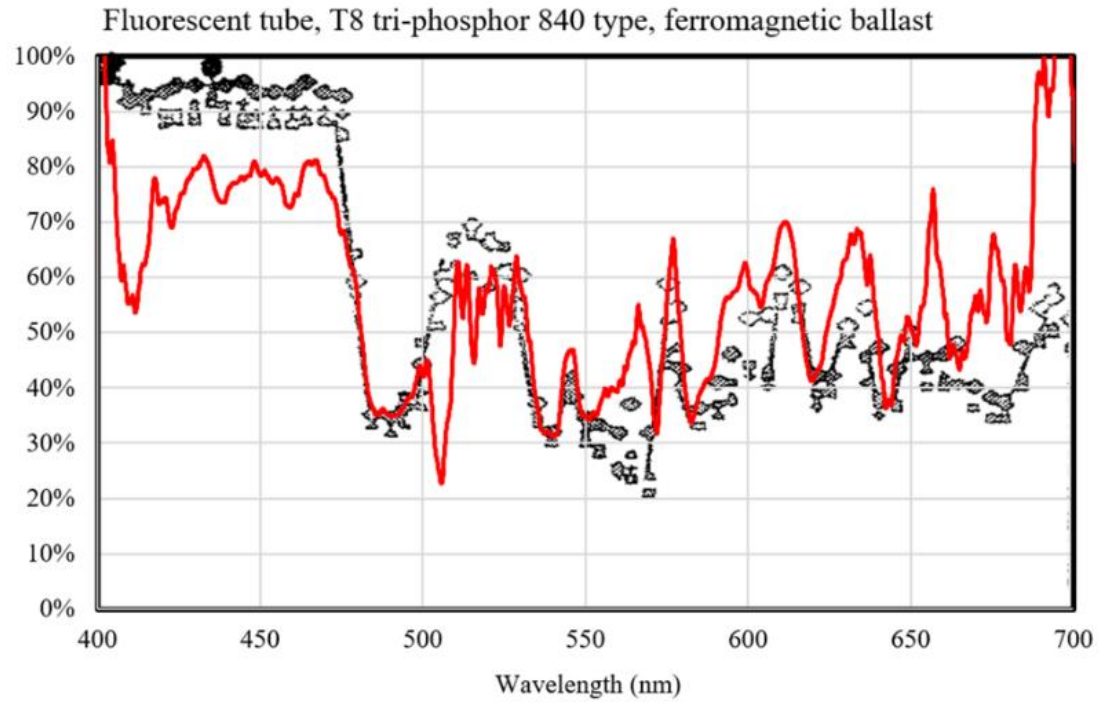

Figure 10, the experimental data are plotted together with graphs adapted from Wilkins and Clark.

Author's version of the following published article:
Martinsons C, Picard N, and Carré S. "Optical Lock-in Spectrometry Reveals Useful Spectral Features of Temporal Light Modulation in Several Light Source Technologies." *LEUKOS*, June 22, 2022, 1–19. https://doi.org/10.1080/15502724.2022.2077754.

To approach their experimental conditions, a moving average filter with a 5 nm bandwidth was applied to our spectral modulation data.

The data concerning the halophosphate tube are in good agreement, although a deviation above 680 nm is observed, a region where our signals become too weak to give reliable spectral modulation values.

The data gathered on the tri-phosphor tube are not in a similar agreement, although both data sets agree on a higher modulation below 480 nm. Above 480 nm, a series of peaks is present of both sets of results, but the peaks are not perfectly aligned in the two measurements. This is a hint that the tested tri-phosphor tube (a recent model bought in 2019) might have a different luminophore composition that the tubes tested in 1990 by Wilkins and Clark. The deviation of our data in the red part of the spectrum is also observed, like in the results of the halophosphate tube.

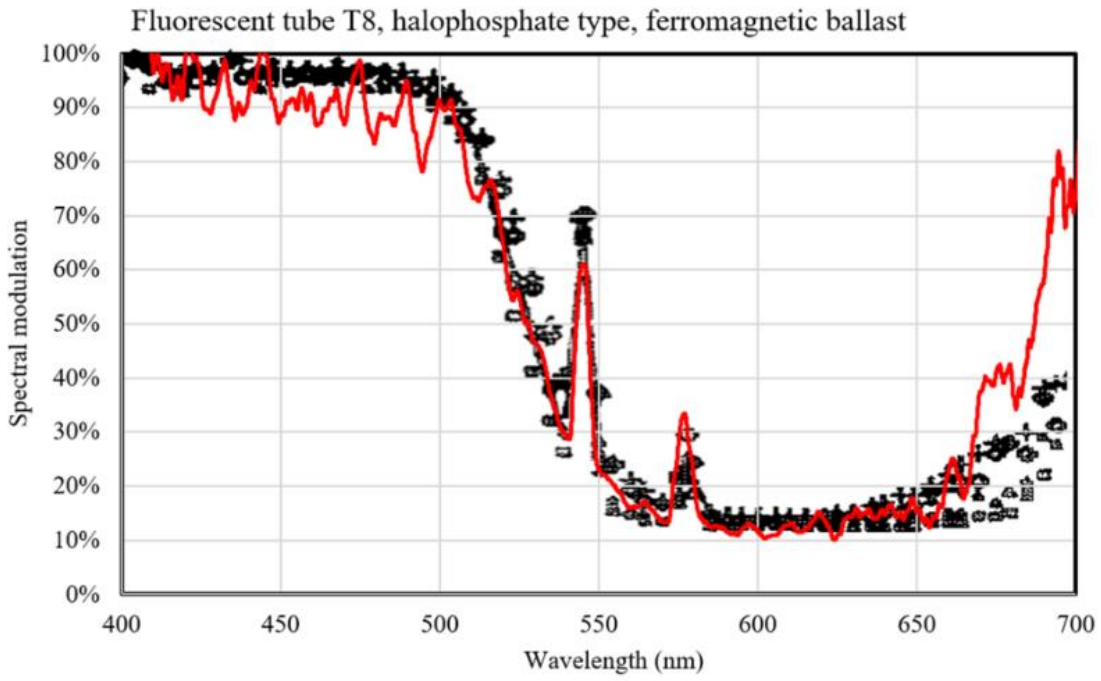

Figure 9. Spectral modulation data measured in this work on a halophosphate fluorescent tube (red solid line) and data published in (Wilkins and Clark 1990) (multiple grey points corresponding to several different tested models).

Author's version of the following published article:
Martinsons C, Picard N, and Carré S. "Optical Lock-in Spectrometry Reveals Useful Spectral Features of Temporal Light Modulation in Several Light Source Technologies." *LEUKOS*, June 22, 2022, 1–19. https://doi.org/10.1080/15502724.2022.2077754.

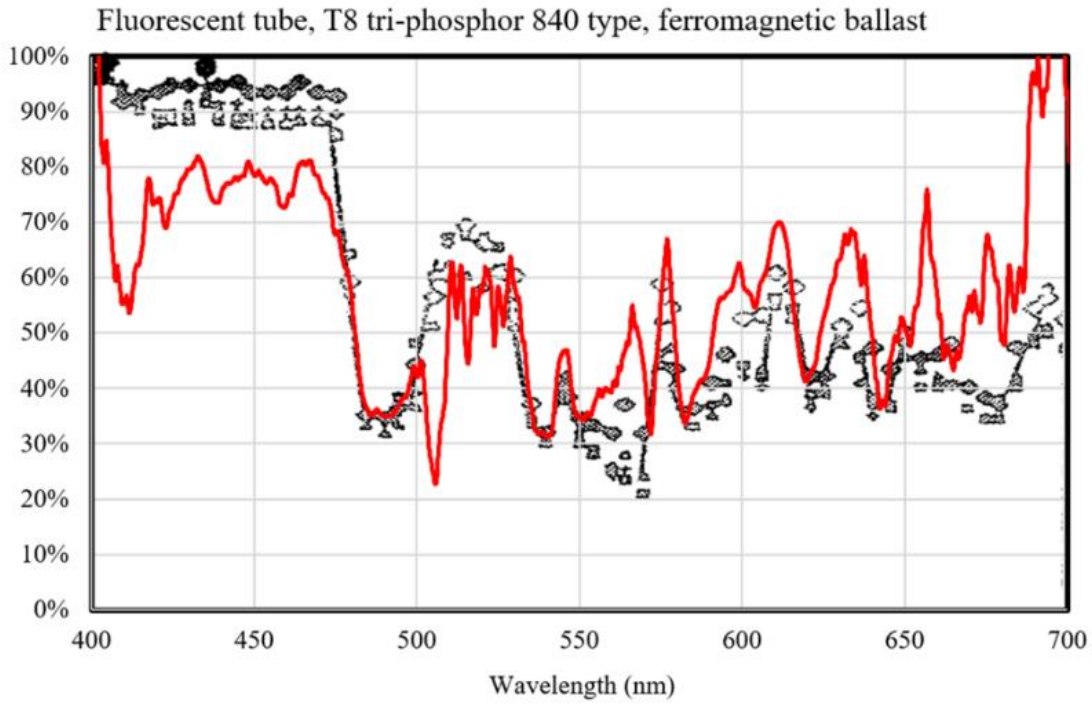

Figure 10. Spectral modulation data measured in this work on a tri-phosphor fluorescent tube (red solid line) and data published in (Wilkins and Clark 1990) (multiple grey points corresponding to several different tested models).

5.2.4.Compact fluorescent lamp (CFL)

The tested CFL uses an integrated electronic ballast operating at high modulation frequency, greater than 20 kHz. However, there is a moderate level of temporal modulation at 100 Hz of about 8% allowing lock-in measurement to be performed at this frequency.

The shape of the spectral distribution of this lamp is similar to the one observed with the tri-phosphor tube, revealing the presence of the same families of luminophore in both types of lamps. The optical lock-in spectrometry operating at 100 Hz gave the results shown in

Author's version of the following published article:
Martinsons C, Picard N, and Carré S. "Optical Lock-in Spectrometry Reveals Useful Spectral Features of Temporal Light Modulation in Several Light Source Technologies." *LEUKOS*, June 22, 2022, 1–19. https://doi.org/10.1080/15502724.2022.2077754.

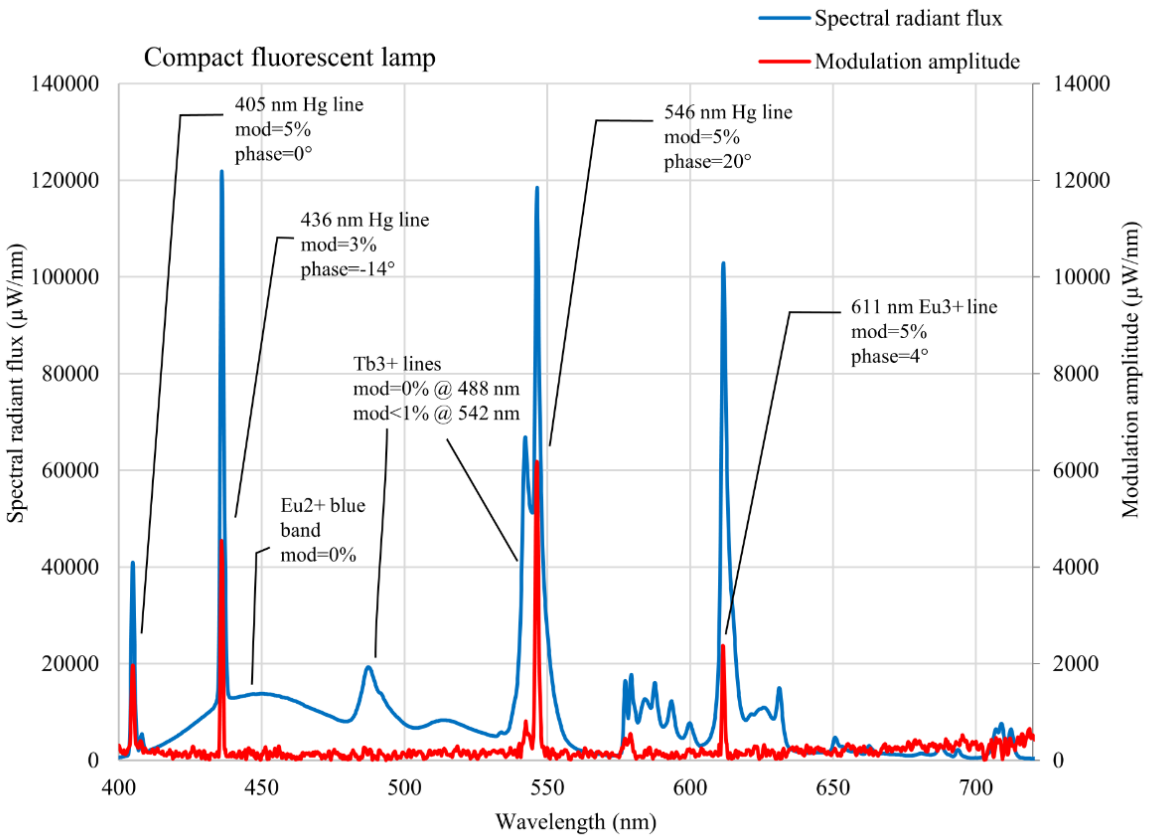

Figure 11. In this figure, the scale of the modulation amplitude is ten times greater than the scale of the spectral radiant flux, for a better clarity of the spectra.

Author's version of the following published article:
Martinsons C, Picard N, and Carré S. "Optical Lock-in Spectrometry Reveals Useful Spectral Features of Temporal Light Modulation in Several Light Source Technologies." *LEUKOS*, June 22, 2022, 1–19. https://doi.org/10.1080/15502724.2022.2077754.

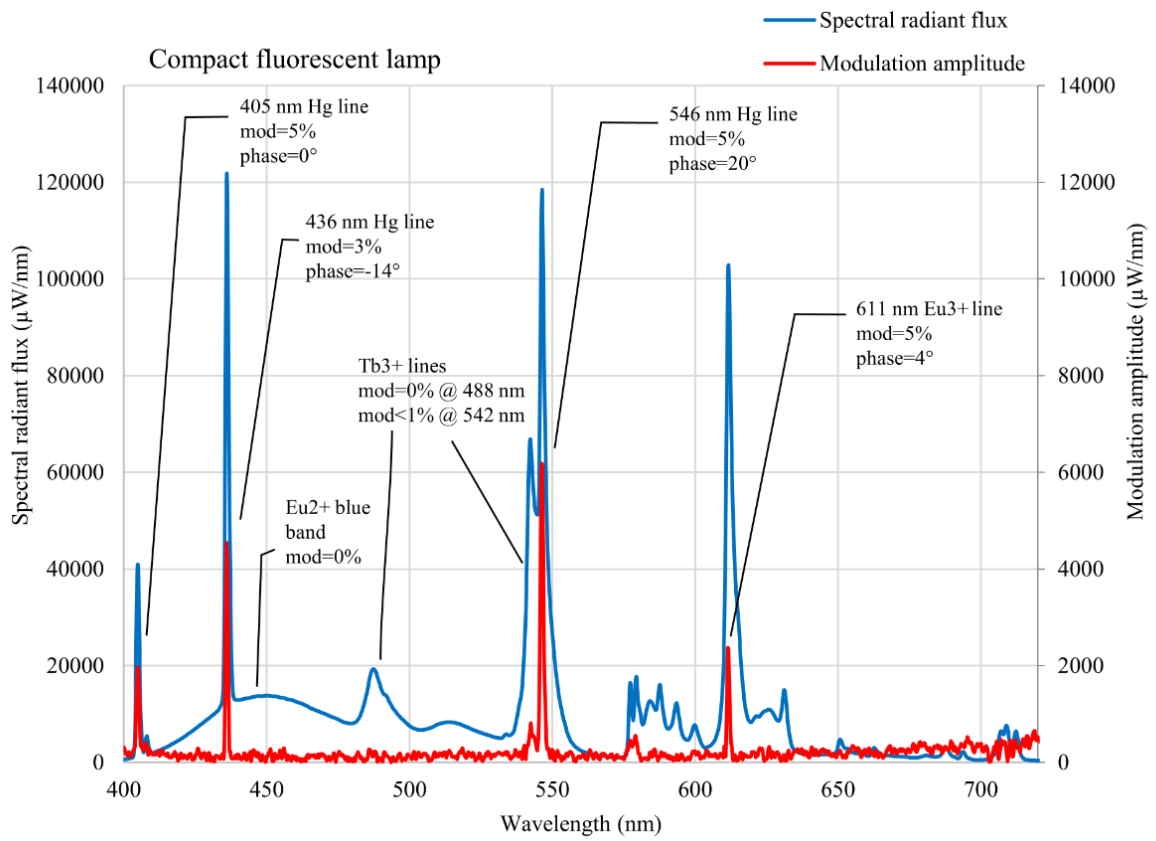

Figure 11. Spectral radiant flux (blue solid line) and modulation amplitude spectrum (red solid line) of the compact fluorescent lamp. The spectral modulation and phase values are reported for the main emission bands.

The mercury lines have a modulation between 3% to 5%. The red emission line of the Eu^{3+} luminophore is modulated at 5%. The most striking characteristic of the amplitude spectrum is that no modulation was detected in the blue-green region between 440 nm and 540 nm, meaning that the luminophores Eu^{2+} and Tb^{3+} emitting in this spectral range have a long lifetime compared with the modulation period of 10 ms. In the other half of the visible range (above 580 nm), the modulation is essentially present in the Eu^{3+} line at 611 nm. The estimation of the fluorescent lifetime of the luminophores of the tested compact fluorescent lamp was not possible because the modulation and phase values were too small. Lock-in measurements at higher frequencies, or at harmonic frequencies of 100 Hz, would be necessary for this purpose.

5.2.5.Discussion about the results obtained on fluorescent lamps

The amplitude and phase spectra measured on the tested fluorescent lamps confirm well-known characteristics concerning the temporal light modulation of this lighting technology. The spectral modulation data measured on a halophosphate tube and a tri-phosphor tube agree fairly well with the data published in (Wilkins and Clark 1990). The optical lock-in spectrometry significantly improves the spectral resolution of the modulation amplitude while keeping measurement times

short - about a few seconds - in comparison with previously used monochromator-based measurement techniques.

The measured modulation amplitude spectra show the influence of the fluorescence lifetime of the luminophore species. In a given emission band, a lower modulation and a greater phase correspond to a longer lifetime. Using our phase and modulation measurements, the estimation of these lifetimes was done assuming a single exponential fluorescence decay. This estimation was only possible in a limited range of lifetimes (between about 0.5 ms to 3 ms). A more accurate estimation of fluorescence lifetimes could be achieved by using several modulation frequencies, including higher frequencies, as done in frequency-domain fluorometry.

The modulated light of fluorescent lamps has different spectral features than the steady-state spectral distribution. For example, the tested CFL lamp had no 100 Hz modulation in the green part of the spectrum. Wilkins and Clark (Wilkins and Clark 1990) noticed that the visual stimuli associated with the spectral modulation of fluorescent lamps were different in comparison with steady-state conditions. Veitch and McColl also considered this effect in their work published in 1995 (Veitch and McColl 1995).

5.3. LED lamps

This section is focused on LED consumer lamps used for indoor residential lighting. Two types of LED technologies were tested: white phosphor-converted LEDs (pc-LED) and tunable RGB LEDs based on three individual color LEDs. White pc-LEDs are now used in the vast majority of LED lamps and luminaires. Tunable RGB LED lamps and luminaires are used in decorative, architectural and façade lighting.

5.3.1. White pc-LED lamp

The results reported here were obtained with a very common type of white pc-LED based on a chip-on-board LED module. The results of the lock-in measurements at 100 Hz are shown in

Author's version of the following published article:
Martinsons C, Picard N, and Carré S. "Optical Lock-in Spectrometry Reveals Useful Spectral Features of Temporal Light Modulation in Several Light Source Technologies." *LEUKOS*, June 22, 2022, 1–19. https://doi.org/10.1080/15502724.2022.2077754.

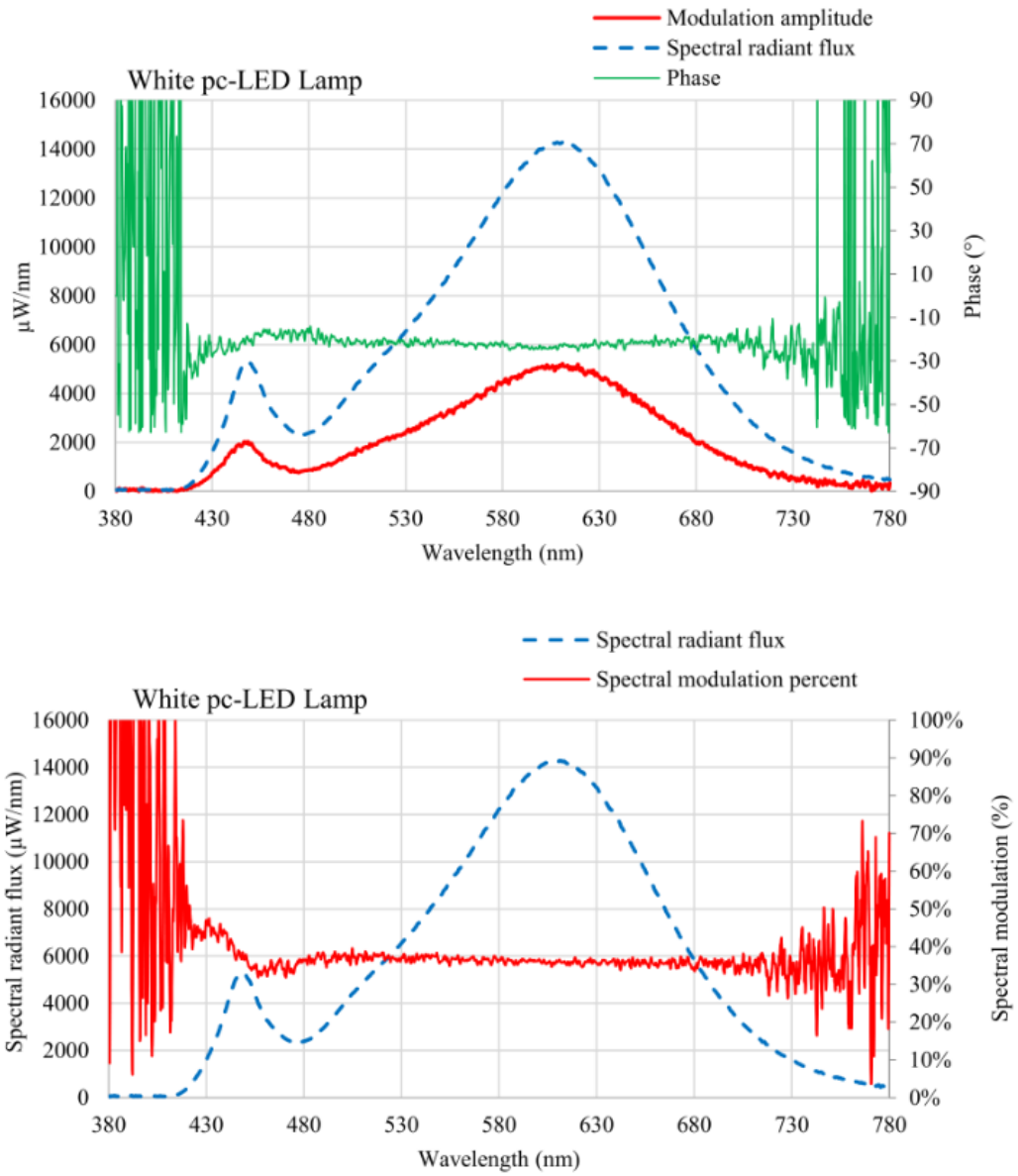

Figure 12. The phase and spectral modulation are well-defined between 410 nm and 750 nm.

The modulation amplitude spectrum closely follows the distribution of the spectral radiant flux. The spectral modulation is indeed almost constant across the emission spectrum. The only significant variation in the spectral modulation occurs around the blue emission band of the LED, where the modulation decreases from 43% to 33% across the blue peak. This slight change in spectral modulation across the blue emission band has also been observed in several other white pc-LED lamps, including filament lamps, tested during the same measurement campaign. Similarly, the phase spectrum of the white pc-LED lamp is nearly flat throughout the visible range, except for a very small variation across the blue emission band, also noticed in other LED lamps of the same technology.

Author's version of the following published article:
Martinsons C, Picard N, and Carré S. "Optical Lock-in Spectrometry Reveals Useful Spectral Features of Temporal Light Modulation in Several Light Source Technologies." *LEUKOS*, June 22, 2022, 1–19. https://doi.org/10.1080/15502724.2022.2077754.

The lock-in measurement at 100 Hz are not sensitive at all to the fluorescence lifetimes of the luminophores of white pc-LEDs. This was expected as these luminophores are YAG:Ce compounds having very short fluorescence lifetimes, of the order of the µs or the ns (Rohwer and Srivastava 2003).

Color parameters were calculated from the modulation amplitude spectrum and compared with the same color parameters calculated from the spectral radiant flux. The chosen color parameters are the correlated color temperature (CCT), the chromaticity coordinates x and y, the color rendering indices Ra and R9. These parameters are used in the latest EU eco-design regulation on lighting products. The results are shown in Table 4. The color parameters calculated from the modulation amplitude spectrum are very close to the standard color parameters calculated from the spectral radiant flux distribution. The deviations are of the same order of magnitude than the typical uncertainties usually associated with the standard measurement of these parameters (Ohno et al. 2014). Consequently, the optical lock-in spectrometry has the ability to perform spectral and color measurements of white pc-LED using the modulation amplitude spectrum.

Table 4. Estimation of color parameters of the pc-white LED lamp from the spectral radiant flux distribution (standard calculation) and from the modulation amplitude spectrum.

Spectral distribution	CCT	x	y	CRI	R9
Spectral radiant flux	2742 K	0.4556	0.4081	84	21
Modulation amplitude spectrum	2790 K	0.4521	0.4078	83	20

Author's version of the following published article:
Martinsons C, Picard N, and Carré S. "Optical Lock-in Spectrometry Reveals Useful Spectral Features of Temporal Light Modulation in Several Light Source Technologies." *LEUKOS*, June 22, 2022, 1–19. https://doi.org/10.1080/15502724.2022.2077754.

Deviation	48 K	-0.0035	-0.0003	-1	-1

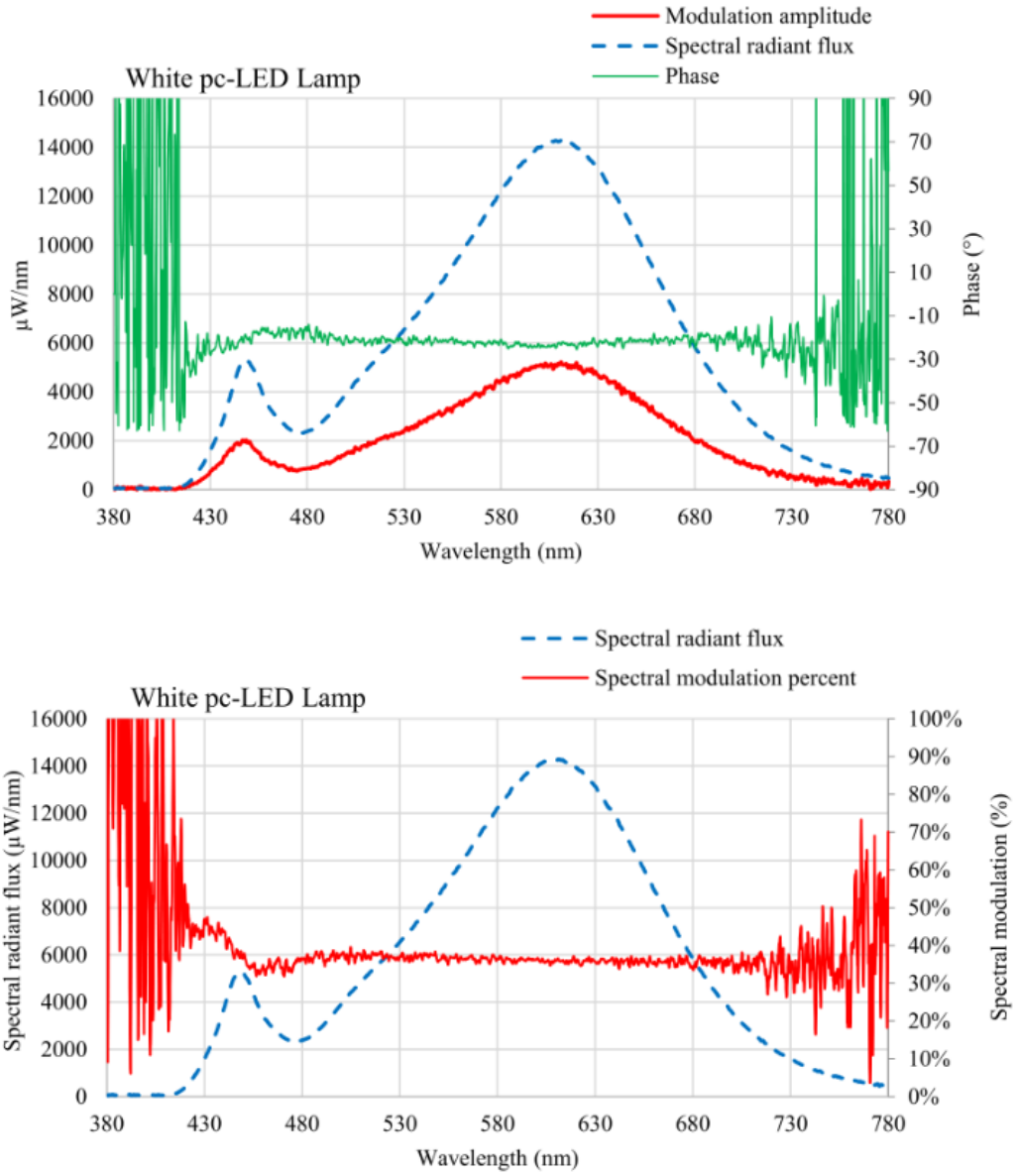

Figure 12. The upper graph shows the spectral radiant flux (dashed blue line) the amplitude (red line) and phase (green line) spectra of the tested white pc-LED lamp. The bottom graph shows the spectral radiant flux (dashed blue line) and the spectral modulation (red line).

5.3.2.Tunable RGB LED lamp

Tunable RGB LED lamps are increasingly used in homes for ambiance lighting. They incorporate at least three different color LEDs, individually controlled by pulse-width modulation (PWM). The

Author's version of the following published article:
Martinsons C, Picard N, and Carré S. "Optical Lock-in Spectrometry Reveals Useful Spectral Features of Temporal Light Modulation in Several Light Source Technologies." *LEUKOS*, June 22, 2022, 1–19. https://doi.org/10.1080/15502724.2022.2077754.

output color and intensity are the result of the additive mixing of the individual color channels operating at adjustable levels. Unlike the previously tested lamps, the temporal light modulation of tunable RGB LED lamps is not the consequence of the AC power supply but is directly associated with PWM.

The results presented here were collected on a lamp model controlled with a smartphone using a WiFi connection. The user interface gave the possibility to set the respective levels of the red, green, and blue LEDs using numbers ranging from 0 to 255. Several settings were tested, and the measured modulation frequency was always 486 Hz, the frequency used by the PWM driving circuit of this lamp.

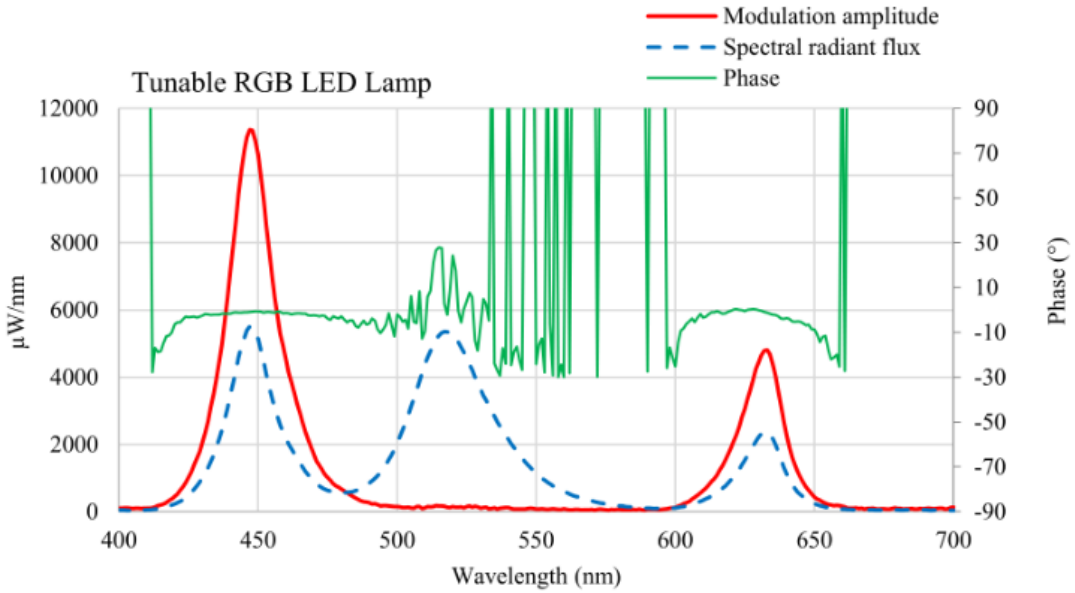

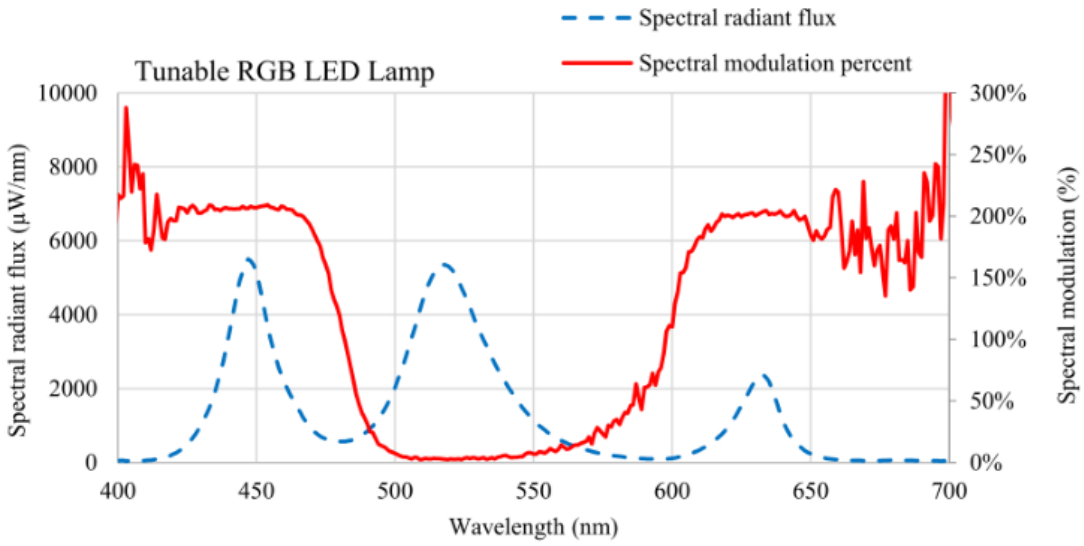

Author's version of the following published article:
Martinsons C, Picard N, and Carré S. "Optical Lock-in Spectrometry Reveals Useful Spectral Features of Temporal Light Modulation in Several Light Source Technologies." *LEUKOS*, June 22, 2022, 1–19. https://doi.org/10.1080/15502724.2022.2077754.

Figure 13 presents the results obtained with a particular setting in which the green channel was adjusted at the maximum level of 255, while the red and blue channels were set at lower levels (red = 51, blue = 81). The measured light waveform (reported in

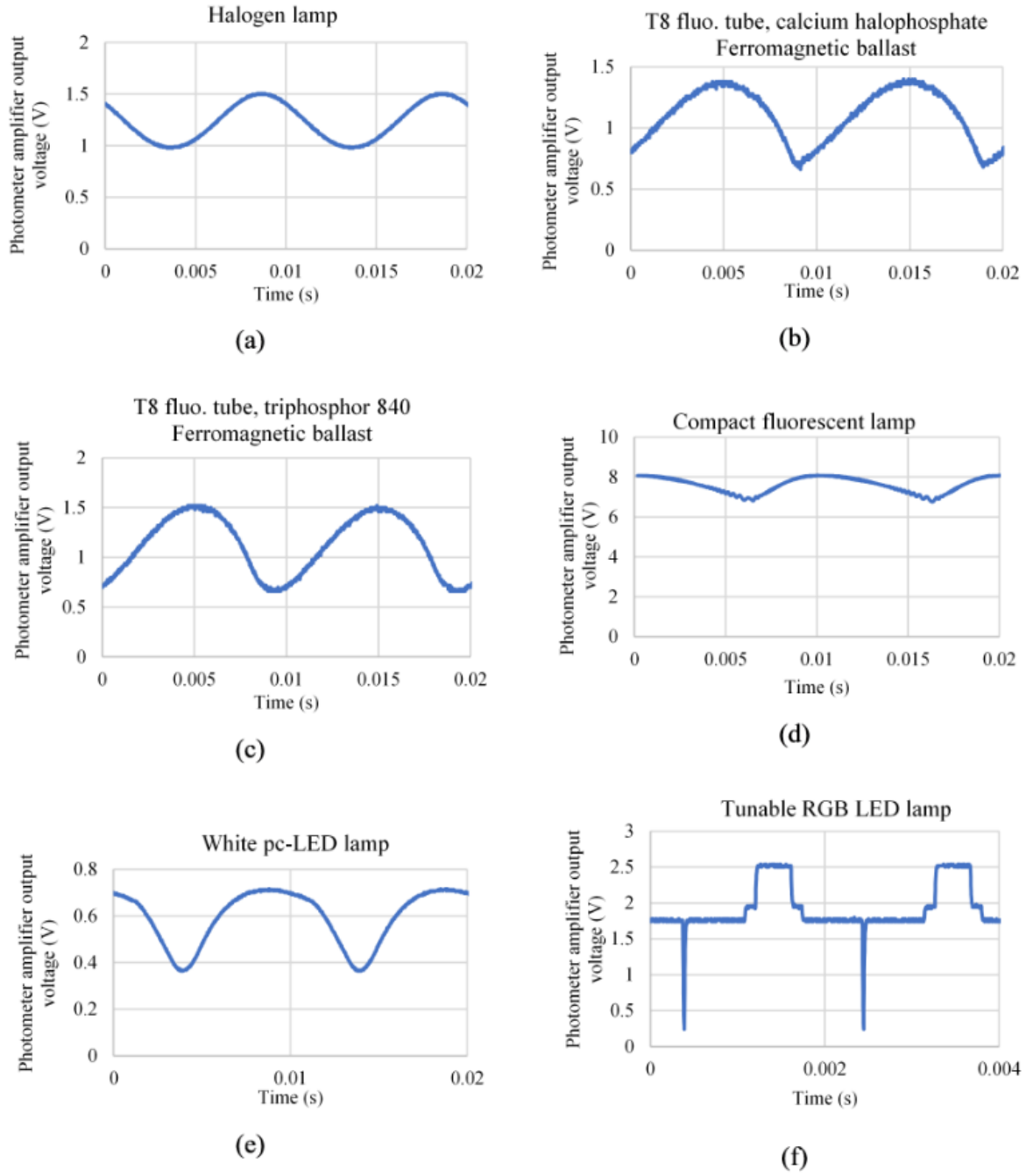

Figure 5) is the superposition of three individual square waves with different duty cycles. The square wave corresponding to the green channel had a duty cycle slightly less than 1, producing an almost constant background level. The two other square waves composing the waveform had different duty cycles, each being less than 0.5.

Author's version of the following published article:
Martinsons C, Picard N, and Carré S. "Optical Lock-in Spectrometry Reveals Useful Spectral Features of Temporal Light Modulation in Several Light Source Technologies." *LEUKOS*, June 22, 2022, 1–19. https://doi.org/10.1080/15502724.2022.2077754.

The measured spectral radiant flux exhibited the three distinct emission bands of the red, blue and green individual LEDs. In the chosen setting, the lock-in measurements show the absence of signal in the modulation amplitude spectrum between roughly 500 nm and 600 nm.

In the blue and red emission bands, the modulation amplitude is greater than the spectral radiant flux. The spectral modulation reaches about 200% in these bands. These values are consistent with the definition of the amplitude which is based on the Fourier coefficient of the temporal light waveform. The temporal light waveforms of the blue and red LEDs being square waves with low duty cycle, their respective Fourier coefficients have a greater value than the amplitude of the waveform.

The measured phase values of the two modulated emission bands (red and blue) of the tested lamp are identical. Measurements performed with other color and intensity settings showed that the three channels always operate with the same phase.

Because of PWM, tunable RGB lamps can generate very different temporal light modulation levels and waveform shapes according to the color and intensity settings. Each setting generally produces a modulation amplitude spectrum different from the steady-state spectral radiant flux.

Author's version of the following published article:
Martinsons C, Picard N, and Carré S. "Optical Lock-in Spectrometry Reveals Useful Spectral Features of Temporal Light Modulation in Several Light Source Technologies." *LEUKOS*, June 22, 2022, 1–19. https://doi.org/10.1080/15502724.2022.2077754.

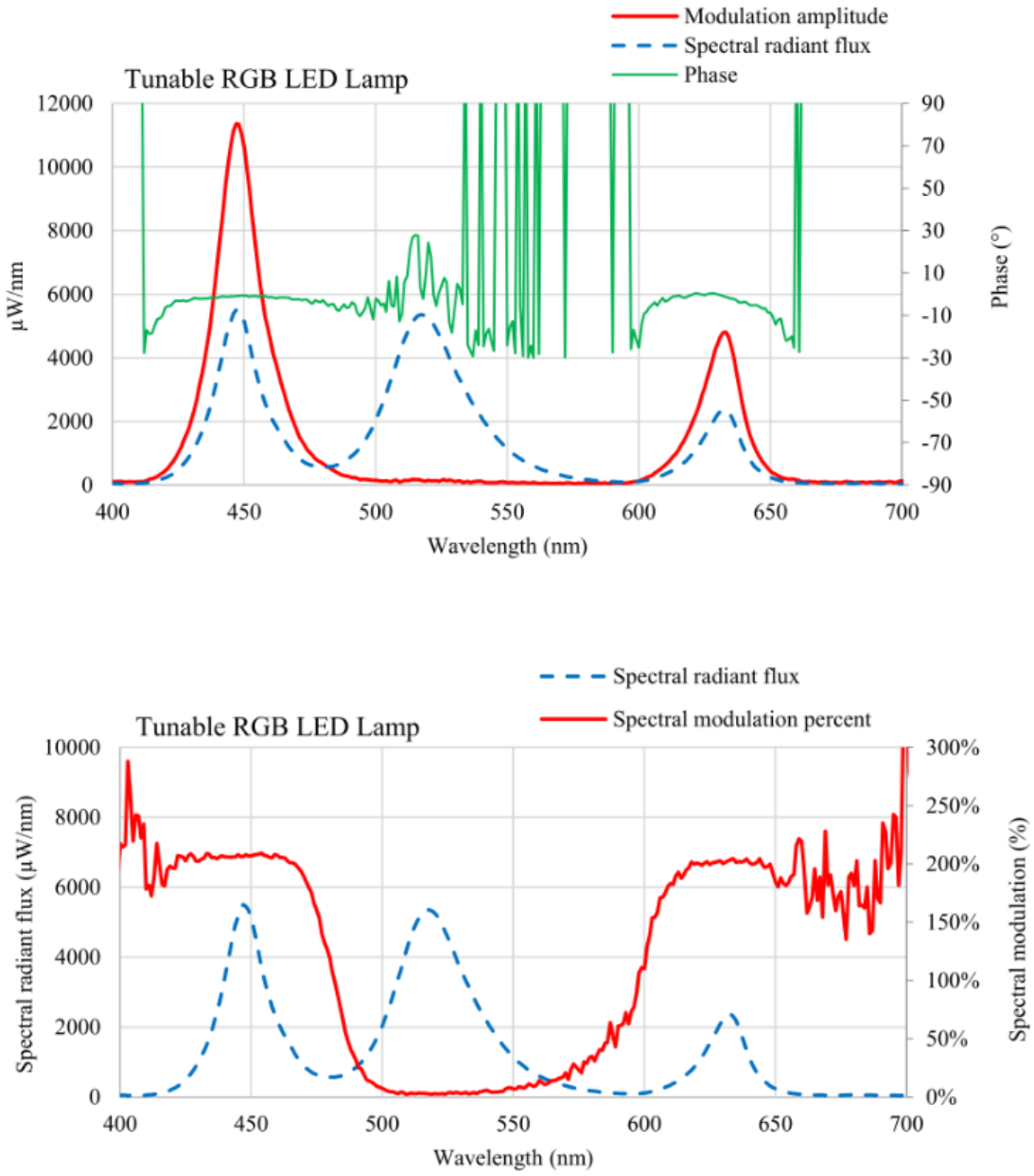

Figure 13. The upper graph shows the spectral radiant flux (dashed blue line) the amplitude (red line) and phase (green line) spectra of the tested tunable RGB LED lamp. The bottom graph shows the spectral radiant flux (dashed blue line) and the spectral modulation (red line).

6. Conclusions

The optical lock-in spectrometry technique described in this paper successfully provided spectral measurements of the amplitude and phase of the temporal light modulation of light sources used in lighting applications. The current implementation of this technique is done in a photometry test laboratory using an integrating sphere. Modulation amplitude and phase spectra were measured at the fundamental modulation frequency in the whole visible range with a resolution of about 1 nm and an acquisition time of a few seconds.

Experimental results were reported for several lamp technologies used in indoor lighting. The results were well correlated with the physical light emission processes involved in each specific technology. For incandescent lamps, the spectral modulation followed a $1/\lambda$ relationship. This smooth and regular variation is explained by the theory of blackbody radiation with a modulated thermal emitter. Using Planck's formula, a simple model was derived to fit the experimental data in order to estimate the amplitude of the temperature oscillation of the lamp filament.

In the case of fluorescent lamps, measurements performed on a halophosphate tube and a tri-phosphor tube - both driven by a ferromagnetic ballast - showed good agreement with spectral modulation data published in 1990 on similar lamps. The spectral modulation of a modern compact fluorescent lamp with an integrated electronic ballast was also reported. The modulation and phase spectra of fluorescent lamps revealed a highly variable spectral modulation rate across the visible range. The highest modulation levels corresponded to the mercury emission lines. The emission bands of the different luminophores had specific amplitude and phase levels, directly related to their fluorescence lifetime. The fluorescence lifetimes could be roughly estimated from our data using a model of single exponential decay. However, the estimation of the fluorescent lifetimes was not the purpose of the optical lock-in spectrometry technique described here. Multiple modulation frequencies would be needed to perform accurate lifetime measurements, as done in frequency-domain fluorometry measurements.

In the case of white phosphor-converted LED lamps, the modulation amplitude and phase spectra recorded at 100 Hz were nearly constant across the visible spectrum, despite the presence of a small oscillation across the blue emission band. We demonstrated that spectral and color parameters of white pc-LEDs could be assessed using the modulation amplitude spectral distribution. This result opens promising opportunities to perform spectrophotometric measurements of LEDs in lock-in mode, thereby providing a rejection of background light, especially useful in field measurements.

The modulation amplitude spectrum measured with a tunable RGB LED lamp is highly dependent on the color and intensity settings chosen by the user. In most settings, it is different from the steady-state spectral radiant flux distribution. This lighting technology may produce temporal color artifacts in human vision if the modulation parameters are not carefully chosen. As reported by Bullough and Skinner (Bullough and Skinner 2019), an illumination provided by this type of lighting caused color artifacts in association with the stroboscopic effect perceived when the observer moved their hands or a small rod. Another type of temporal light artifact can be perceived with this lamp technology: the phantom array effect. The phantom array is a series of multiple ghost images of a modulated

light source appearing during eye saccades (Hershberger and Jordan 1998). The spectral modulation of PWM RGB LEDs may "color" the ghost images, creating a color breakup phenomenon, like what is seen on displays presenting colors sequentially (Johnson, Kim, and Banks 2014).

More work should be carried out to improve the technical capabilities of the optical lock-in spectrometry technique described in this paper. The current four-port modulation unit is very efficient but limited to frequencies below 1000 Hz. Furthermore, this unit is not portable and cannot be used in field measurements. The first improvement would be to operate without a four-port modulation unit by using synchronized time-gated acquisitions of spectral data directly triggered by the reference signal using the control functions of the array spectrometers. This would allow the two spectrometers to work in lock-in mode without the need of an external modulation unit. Measurements at higher frequencies (or at harmonic frequencies of the fundamental modulation frequency) could be achieved in the laboratory and in field measurements.

A chopper-less optical lock-in spectrometry instrument could be used to perform field measurements of modulated light sources in association with either an irradiance head, an objective lens, or a telescope. Several types of measurements would benefit from the optical lock-in mode:

- Spectrophotometric measurements of indoor LED lighting in the presence of daylight and background light
- Remote sensing of outdoor LED luminaires to test the compliance of their spectral power distribution with local light pollution regulations
- Non-destructive evaluation of light-emitting diodes and laser diodes during a continuous pulse method, by acquiring the lock-in amplitude and phase spectra at the repetition frequency of the current pulses.

In addition to lighting, the optical lock-in spectrometry technique described in this paper could be applied to improve measurements in other areas such as:

- Non-contact spectral reflectance measurements using a modulated illumination beam to reject background light and differentiate reflected signals from signals produced by the fluorescence of the sample under test
- Differential optical absorption spectrometry (DOAS) long-path measurements of urban air pollutants such as NO_2 using outdoor lighting LED luminaires as temporally modulated light sources

- Analytical optical spectrometry (absorption and Raman spectrometry for instance) using modulated beams
- Frequency-domain spectrofluorometry
- Photothermal techniques such as multi-wavelengths radiation thermometry, laser absorption radiation thermometry, and lock-in infrared thermography.

This work can be concluded by remarking that a low to moderate level of temporal light modulation can help improve spectrophotometric and color measurements of solid-state lighting through lock-in detection. Of course, promoting the use of temporal light modulation is only possible if its impacts are correctly assessed and if the resulting risk levels for health, safety and the environment are acceptable.

7. Acknowledgement

The authors are grateful to Prof. Geneviève Chadeyron of the SIGMA Clermont Institute for fruitful discussions concerning luminophores used in lighting applications.

8. Funding

This work was entirely funded by the Centre Scientifique et Technique du Bâtiment (CSTB) through the internal research program "Indoor Environmental Quality: Measurements and Modeling".

9. Disclosure Statement

No potential conflict of interest was reported by the authors.

10. References

Bullough, John D., and Nicholas P. Skinner. 2019. 'Investigation of Stroboscopic Effects from Chromatic Flicker'. In *Proceedings of the 29th Quadrennial Session of the CIE*, 1605–12. Washington DC, https://doi.org/10.25039/x46.2019.PO161.

Cao, Huy Tuong, Daniel D. Brown, Peter J. Veitch, and David J. Ottaway. 2020. 'Optical Lock-in Camera for Gravitational Wave Detectors'. *Optics Express* 28 (10): 14405. https://doi.org/10.1364/OE.384754.

CIE. 2016. 'Visual Aspects of Time-Modulated Lighting Systems – Definitions and Measurement Models'. CIE TN 006. Commission Internationale de l'Eclairage (CIE).

Author's version of the following published article:
Martinsons C, Picard N, and Carré S. "Optical Lock-in Spectrometry Reveals Useful Spectral Features of Temporal Light Modulation in Several Light Source Technologies." *LEUKOS*, June 22, 2022, 1–19. https://doi.org/10.1080/15502724.2022.2077754.

CIE. 2021. 'Guidance on the Measurement of Temporal Light Modulation of Light Sources and Lighting Systems'. CIE TN 012. Commission Internationale de l'Eclairage (CIE). https://doi.org/10.25039/TN.012.2021.

CIE. 2022. 'Visual Aspects of Time-Modulated Lighting Systems'. CIE 249:2022. Commission Internationale de l'Eclairage. https://doi.org/10.25039/TR.249.2022.

DiLaura, David L, Kevin W. Houser, Richard G. Mistrick, and Gary R. Steffy. 2011. *The Lighting Handbook Tenth Edition, Reference and Applications*. New York, NY: Illuminating Engineering Society.

Fodor, P. S., S. Rothenberger, and J. Jevy. 2005. '320-Channel Dual Phase Lock-in Optical Spectrometer'. *Review of Scientific Instruments* 76 (1): 013103. https://doi.org/10.1063/1.1830013.

Hartmann, Jurgen. 2006. 'Correct Consideration of the Index of Refraction Using Blackbody Radiation'. *Optics Express* 14 (18): 8121. https://doi.org/10.1364/OE.14.008121.

Hershberger, Wayne A., and J. Scott Jordan. 1998. 'The Phantom Array: A Perisaccadic Illusion of Visual Direction'. *The Psychological Record* 48 (1): 21–32. https://doi.org/10.1007/BF03395256.

Johnson, Paul V., Joohwan Kim, and Martin S. Banks. 2014. 'The Visibility of Color Breakup and a Means to Reduce It'. *Journal of Vision* 14 (14): 10. https://doi.org/10.1167/14.14.10.

Ohno, Yoshi, Koichi Nara, Elena Revtova, Wei Zhang, Tastuya Zama, and C. Cameron Miller. 2014. 'Solid State Lighting Annex: 2013 Interlaboratory Comparison. Final Report.' International Enery Agency 4E Implementing Agreement, Solid-State Lighting Annex.

Ragni, A., G. Sciortino, M. Sampietro, G. Ferrari, F. Crisafi, V. Kumar, and D. Polli. 2018. 'Lock-In Based Differential Front-End For Raman Spectroscopy Applications'. In *2018 14th Conference on Ph.D. Research in Microelectronics and Electronics (PRIME)*, 221–24. Prague: IEEE. https://doi.org/10.1109/PRIME.2018.8430339.

Rohwer, Lauren Shea, and Alok Srivastava. 2003. 'Development of Phosphors for LEDs'. *The Electrochemical Society Interface* 12 (2): 36–39. https://doi.org/10.1149/2.F09032IF.

Sekulovski, D, S Poort, M Perz, and L Waumans. 2019. 'Effects of Long-Term Exposure to Stroboscopic Effect from Moderate-Level Modulated Light'. *Lighting Research & Technology*, 147715351988147. https://doi.org/10.1177/1477153519881473.

Van der Horst, Gerard J. C. 1969. 'Chromatic Flicker'. *Journal of the Optical Society of America* 59 (9): 1213. https://doi.org/10.1364/JOSA.59.001213.

Veitch, Jennifer A, Martinsons C, Coyne S, and Dam-Hansen C. 2021. 'Correspondence: On the State of Knowledge Concerning the Effects of Temporal Light Modulation'. *Lighting Research & Technology* 53 (1): 89–92. https://doi.org/10.1177/1477153520959182.

Veitch, Jennifer A, and Shelley L McColl. 1995. 'Modulation of Fluorescent Light: Flicker Rate and Light Source Effects on Visual Performance and Visual Comfort'. *Lighting Research and Technology* 27 (4): 243–56. https://doi.org/10.1177/14771535950270040301.

Vetromile, Carissa M., and David M. Jameson. 2014. 'Frequency Domain Fluorometry: Theory and Application'. In *Fluorescence Spectroscopy and Microscopy*, edited by Yves Engelborghs and Antonie J.W.G. Visser, 1076:77–95. Methods in Molecular Biology. Totowa, NJ: Humana Press. https://doi.org/10.1007/978-1-62703-649-8_5.

Wang, Jingru, Zhihong Wang, Xufei Ji, Jie Liu, and Guangda Liu. 2017. 'A Simplified Digital Lock-in Amplifier for the Scanning Grating Spectrometer'. *Review of Scientific Instruments* 88 (2): 023101. https://doi.org/10.1063/1.4974755.

Wilkins, A.J., and C. Clark. 1990. 'Modulation of Light from Fluorescent Lamps'. *Lighting Research & Technology* 22 (2): 103–9. https://doi.org/10.1177/096032719002200205.

Zurich Instrument. 2016. 'White Paper: Principles of Lock-in Detection and the State of the Art'. Zurich Instruments. https://www.zhinst.com/europe/en/resources/principles-of-lock-in-detection.

Srivastava, Alok, and C.R. Ronda. 2003. "Phosphors." The Electrochemical Society Interface 12, no. 2 (June 1, 2003): 48–51.